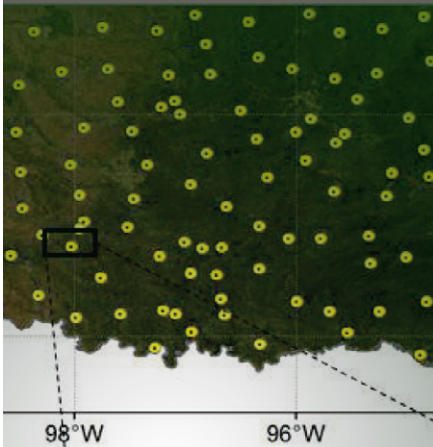


Special Section: Remote Sensing  
for Vadose Zone Hydrology

Bin Fang\*  
Venkat Lakshmi  
Rajat Bindlish  
Thomas J. Jackson  
Michael Cosh  
Jeffrey Basara



A soil moisture downscaling algorithm based on the thermal inertia relationship between daily temperature changes and daily average soil moisture is presented and the remote sensed products skin surface temperature and vegetation index are used. The downscaled soil moisture estimates are applied to the passive microwave radiometer AMSR-E soil moisture for enhancing its spatial resolution to 1 km.

Bin Fang, Venkat Lakshmi, Department of Earth and Ocean Sciences, University of South Carolina, Columbia, SC 29208; Rajat Bindlish, Thomas J. Jackson, Michael Cosh, Hydrology and Remote Sensing Laboratory, Beltsville Agricultural Research Center, United States Department of Agriculture, Beltsville MD 20705; Jeffrey Basara, School of Meteorology, Oklahoma Climate Survey, University of Oklahoma, Norman OK 73072. \*Corresponding author (bfang@geol.sc.edu).

Vadose Zone J.  
doi:10.2136/vzj2013.05.0089  
Received 1 July 2013.

© Soil Science Society of America  
5585 Guilford Rd., Madison, WI 53711 USA.  
All rights reserved. No part of this periodical may be reproduced or transmitted in any form or by any means, electronic or mechanical, including photocopying, recording, or any information storage and retrieval system, without permission in writing from the publisher.

# Passive Microwave Soil Moisture Downscaling Using Vegetation Index and Skin Surface Temperature

Soil moisture satellite estimates are available from a variety of passive microwave satellite sensors, but their spatial resolution is frequently too coarse for use by land managers and other decision makers. In this paper, a soil moisture downscaling algorithm based on a regression relationship between daily temperature changes and daily average soil moisture is developed and presented to produce an enhanced spatial resolution soil moisture product. The algorithm was developed based on the thermal inertia relationship between daily temperature changes and averaged soil moisture under different vegetation conditions, using  $1/8^\circ$  spatial resolution North American Land Data Assimilation System (NLDAS) surface temperature and soil moisture data, as well as 5-km Advanced Very High Resolution Radiometer (AVHRR) (1981–2000) and 1-km Moderate Resolution Imaging Spectroradiometer (MODIS) Normalized Difference Vegetation Index (NDVI) and surface temperature (2002–present) to build the look-up table at  $1/8^\circ$  resolution. This algorithm was applied to the 1-km MODIS land surface temperature to obtain the downscaled soil moisture estimates and then used to correct the soil moisture products from Advanced Microwave Scanning Radiometer–EOS (AMSR-E). The 1-km downscaled soil moisture maps display greater details on the spatial pattern of soil moisture distribution. Two sets of ground-based measurements, the Oklahoma Mesonet and the Little Washita Micronet, were used to validate the algorithm. The overall averaged slope for 1-km downscaled results vs. Mesonet data is 0.219, which is better than AMSR-E and NLDAS, while the spatial standard deviation ( $0.054 \text{ m}^3 \text{ m}^{-3}$ ) and unbiased RMSE ( $0.042 \text{ m}^3 \text{ m}^{-3}$ ) of 1-km downscaled results are similar to the other two datasets. The overall slope and spatial standard deviation for 1-km downscaled results vs. Micronet data ( $0.242$  and  $0.021 \text{ m}^3 \text{ m}^{-3}$ , respectively) are significantly better than AMSR-E and NLDAS, while the unbiased RMSE ( $0.026 \text{ m}^3 \text{ m}^{-3}$ ) is better than NLDAS and further than AMSR-E. In addition, Mesonet comparisons of all three soil moisture datasets demonstrate a stronger statistical significance than Micronet comparisons, and the  $p$  value of 1-km downscaled is generally better than the other two soil moisture datasets. The results demonstrate that the AMSR-E soil moisture was successfully disaggregated to 1 km. The enhanced spatial heterogeneity and the accuracy of the soil moisture estimates are superior to the AMSR-E and NLDAS estimates, when compared with in situ observations.

Abbreviations: AEF, Actual Evaporative Fraction; AMSR, Advanced Microwave Scanning Radiometer; AMSR2, Advanced Microwave Scanning Radiometer 2; AMSR-E, Advanced Microwave Scanning Radiometer–EOS; ASTER, Advanced Spaceborne Thermal Emission and Reflection Radiometer; AVHRR, Advanced Very High Resolution Radiometer; CMG, Climate Modeling Grid; DisPATCh, Physical And Theoretical scale Change; EASE, Equal-Area Scalable Earth; EF, Evaporative Fraction; LST, Land Surface Temperature; MODIS, Moderate Resolution Imaging Spectroradiometer; NDVI, Normalized Difference Vegetation Index; NLDAS, North American Land Data Assimilation System; SGP, Southern Great Plains; SMAP, Soil Moisture Active Passive Mission; SMOS, Soil Moisture and Ocean Salinity mission.

**Soil moisture remote sensing** has a long history with microwave radiometry. The spatial resolution obtained by a microwave radiometer (hence forth referred to as simply a radiometer) is inversely proportional to the diameter of the antenna and directly proportional to the height of the satellite platform for a given frequency. Higher spatial resolution is desired by a diverse set of fields of application such as agriculture and monitoring and prediction of weather, droughts, and floods. Consequently, to obtain high spatial resolution data one would need a large aperture antenna or a low orbit. Lowering the altitude is undesirable because it reduces temporal frequency and decreases the lifetime of the mission. Solutions to the large antenna limitations are currently being investigated using the Soil Moisture and Ocean Salinity mission (SMOS) by ESA and Soil Moisture Active Passive Mission (SMAP) by NASA, but it remains a problem for many operational systems.

Recognizing the need for improved spatial resolution and the limitations described above, other solutions to improve resolution of soil moisture monitoring should be explored. One

example is SMAP mission (Entekhabi et al., 2008), set for launch in 2014. SMAP will utilize a very large antenna and combined radiometer and radar measurements to provide soil moisture at higher resolutions than radiometers alone can currently achieve. SMAP (Entekhabi et al., 2008) consists of both passive and active microwave sensors. The radiometer will have a nominal spatial resolution of 36 km, and the active radar will have a resolution of 1 km. The active microwave remote sensing data can provide a higher spatial resolution observation of backscatter than those obtained from a radiometer (order of magnitude: radiometer, 40 km; radar, 1 km or better). However, radar data are more strongly affected by local roughness, microscale topography, and vegetation than a radiometer, suggesting that it is difficult to invert backscatter to soil moisture accurately. Therefore, the current radar alone algorithms cannot meet the accuracy requirements of the soil moisture mission ( $0.04 \text{ m}^3 \text{ m}^{-3}$ ). SMAP will use high-resolution radar observations to disaggregate coarse resolution radiometer observations to produce a soil moisture product at 9-km resolution. On the other hand, soil moisture has been retrieved from radiometer data successfully using various sensors and platforms, and these retrieval algorithms have an established heritage (Schmugge et al., 1974; Njoku and Entekhabi, 1996; Lakshmi, 1997).

In this study we implemented an alternative approach to derive higher resolution soil moisture that would complement the SMAP approach and at the same time has the potential to be used immediately with available satellite systems as well as downscaling historical satellite products. This method will help to establish a long-term record of high spatial resolution soil moisture, beginning with the Advanced Microwave Scanning Radiometer (AMSR) instrument, which is on board NASA's Aqua satellite and launched in 2002, and continuing with Advanced Microwave Scanning Radiometer 2 (AMSR2), which is on board JAXA's

GCOM-W1 satellite and launched in 2012 (Imaoka et al., 2010). We propose the use of land surface temperature and vegetation index data derived from two NASA sensors—AVHRR (since the late 1970s) and MODIS—as well as AMSR-E on board the Aqua (2002–2011) spacecraft.

Over the past few years various methods have integrated the use of active sensors with a higher spatial resolution to downscale passive microwave soil moisture retrievals (Narayan et al., 2004; Narayan and Lakshmi, 2008; Das et al., 2011). Recently, numerous studies have addressed the soil moisture downscaling problem using MODIS-sensor derived temperature, vegetation, and other land surface variables. There have been numerous major publications in this area of study. A method based on a “universal triangle” concept was used to retrieve soil moisture from NDVI and Land Surface Temperature (LST) data (Piles et al., 2011). A relationship between surface soil moisture and soil evaporative efficiency was explored for catchment studies in southeastern Australia (Merlin et al., 2010). A method to downscale soil moisture by using two soil moisture indices, Evaporative Fraction (EF) and Actual Evaporative Fraction (AEF), was developed and applied in southeastern Arizona (Merlin et al., 2008a,b). A sequential model using MODIS as well as Advanced Spaceborne Thermal Emission and Reflection Radiometer (ASTER) data was proposed for downscaling soil moisture (Merlin et al., 2009). In addition, Merlin et al. (2012) used the algorithm of Physical And Theoretical scale Change (DisPATCH) to convert high spatial resolution soil temperature from MODIS into soil moisture. They applied this method to disaggregate SMOS soil moisture in southeastern Australia (Merlin et al., 2012). Kim and Hogue (2012) developed an integrated algorithm using enhanced vegetation index and surface temperature derived from MODIS to downscale AMSR-E soil moisture in California and compared their results with several previous downscaling methods (Kim and Hogue, 2012). Table 1

Table 1. Studies on downscaling soil moisture using various remote sensing and modeling techniques.

Author	Methodology	Time and region	Results
Merlin et al. (2010)	Based on the relationship between soil evaporative efficiency and soil moisture	NAFE 2006 (Oct.–Nov.), Yanco, Southeastern Australia	Mean correlation slope between simulated and measured data is 0.94, the most accuracy with an error of $0.012 \text{ m}^3/\text{m}^3$
Piles et al. (2011)	Build model between LST, NDVI and soil moisture	Jan.–Feb. 2010, Murrumbidgee catchment, Yanco, Southeastern Australia	$R^2$ is between 0.14~0.21 and RMSE is between $0.9\sim 0.17 \text{ m}^3 \text{ m}^{-3}$
Merlin et al. (2008a)	Downscaling algorithm is derived from MODIS and physical based soil evaporative efficiency model	NAFE 2006 (Oct.–Nov.), Murrumbidgee catchment, Yanco, Southeastern Australia	Overall RMSE is between 1.4~1.8% (v/v)
Merlin et al. (2008b)	Based on two soil moisture indices EF and AEF	June and August 1990 (Monsoon'90 experiment), USDA-ARS WGEW in southeastern Arizona	Total accuracy is 3% (v/v) for EF and 2% (v/v) for AEF, and correlation coefficient is 0.66~0.79 for EF and 0.71~0.81 for AEF
Merlin et al. (2009)	Sequential model	NAFE 2006 (Oct.–Nov.), Yanco, southeastern Australia	RMSE is $-0.062 \text{ m}^3 \text{ m}^{-3}$ and the bias is $0.045 \text{ m}^3 \text{ m}^{-3}$
Merlin et al. (2012)	Physical And Theoretical scale Change (DisPATCH) method	Jan., Feb. and Sept. 2010, Murrumbidgee catchment, Yanco, Southeastern	The correlation coefficient between disaggregated and in situ soil moisture between 0.70~0.85 in summer
Kim and Hogue (2012)	Enhanced vegetation index and surface temperature derived from MODIS	SMEX04 field measurement from the San Pedro River Basin	Spatial correlation are generally from $-0.08$ to 0.34

lists these studies, the methods, and significant results of the soil moisture downscaling. Furthermore, quite a few of studies have reported using dynamic and three-dimensional data assimilation techniques to develop soil moisture downscaling algorithms (Parada and Liang, 2004; Pan et al., 2009; Sahoo et al., 2012; Zhou et al., 2008).

In our proposed downscaling method, we use the relationship between soil moisture and surface temperature modulated by vegetation. This approach has a background in past studies of Mallick et al. (2009), who used the triangular relationship (Goetz, 1997; Sandholt et al., 2002) between surface temperature and the vegetation index derived from the MODIS Aqua sensor data. From this, they derived the soil wetness index that was converted to soil moisture at a 1-km scale. Minacapilli et al. (2009) used thermal infrared observations from an airborne platform to estimate soil moisture using the thermal inertia principle for a bare soil field. They found that the estimated soil moisture correlated very well with in situ observations. Gillies and Carlson (1995) devised a method that derived the fractional vegetation and spatial patterns of soil moisture using the AVHRR data set and demonstrated this method in a region of England. In our method, the diurnal temperature range was used (Karl, 1984), which was affected by vegetation (Collatz, 2000), soil moisture, and clouds (Dai and Deser, 1999).

## Data Sources

The state of Oklahoma was selected as the study area due to its long history of soil moisture research. The Oklahoma Mesonet and Little Washita River Experimental Watershed Micronet are two long-term in situ soil moisture networks providing a solid foundation for soil moisture remote sensing research (shown in Fig. 1). The Little Washita has been the location for various soil moisture field experiments, including Southern Great Plains (SGP) SGP97, SGP99, and SMEX03 (Jackson et al., 1999; Jackson et al., 2002), and has been a key element in satellite validation studies (Jackson et al., 2010; Mladenova et al., 2011). In addition to the ground resources, a variety of spaceborne sensors also contributed to this study. Descriptions and maps of the datasets used in this article are shown in Table 2 and Fig. 2. Table

2 lists the spatial resolution and temporal repeat of these sensors and their data products.

## NLDAS Data

The North American Land Data Assimilation System (NLDAS, 2011) phase 2 hourly mosaic data is used in this study. NLDAS is run hourly on a geographical grid with a spatial resolution of  $1/8^\circ$  (12.5 km). The NLDAS data output includes various surface variables, such as radiation flux, surface runoff, surface temperature, vegetation indices, and soil moisture (Mitchell et al., 2004). Soil, vegetation, and elevation are parameterized using high resolution datasets (1-km satellite data in the case of vegetation). The forcing data (Cosgrove et al., 2003; Luo et al., 2003) and outputs have been extensively validated (Lohmann et al., 2004; Robock et al., 2003; Schaake et al., 2004). The soil moisture downscaling model included the use of two variables: surface skin temperature and soil moisture at 0 to 10 cm depth. The data used in this study correspond to the closest local overpass times of Aqua satellite for the Oklahoma region, which are approximately 08:00 and 20:00 in UTC time.

## AMSR-E Data

The Advanced Scanning Microwave Radiometer on board the EOS Aqua platform (AMSR-E) collected microwave observations at frequencies of 6, 10, 19, 37, and 85 GHz from 2002 to 2011 (Njoku et al., 2003). The AMSR-E instrument provided global passive microwave measurements of terrestrial, oceanic, and atmospheric

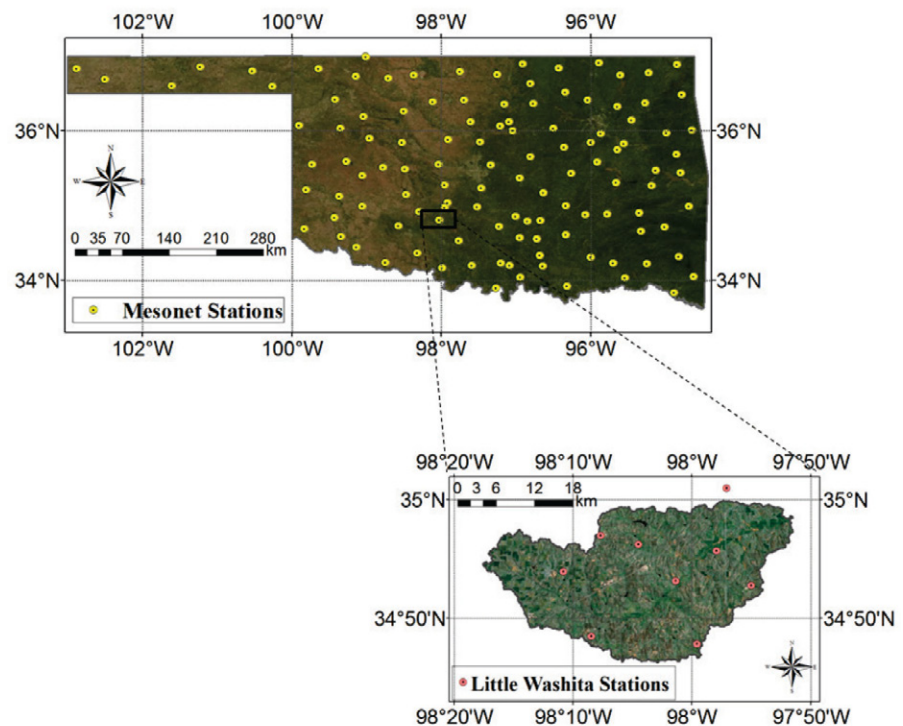


Fig. 1. Imagery Maps of study region of Oklahoma and the Little Washita Watershed. The locations of the Mesonet Stations are denoted in open yellow circles, and the soil moisture sites for Little Washita are noted in red dots.

Table 2. Sources of land surface data used in the downscaling of soil moisture and their spatial resolution and temporal repeat.

Source	Data	Spatial resolution	Temporal repeat
NLDAS	Soil moisture content (0–10 cm layer, kg/m <sup>2</sup> )	1/8° (12.5 km)	hourly
	Surface skin temperature (K)	1/8° (12.5 km)	hourly
AVHRR	Normalized difference vegetation index (NDVI)	5 km	daily
MODIS	Normalized difference vegetation index (NDVI)	5 km	biweekly
	Land surface temperature (K)	1 km	daily
AMSR-E	Soil moisture content (m <sup>3</sup> m <sup>-3</sup> )	1/4° (25 km)	daily
Mesonet	Surface soil moisture content (0–5 cm layer, m <sup>3</sup> m <sup>-3</sup> )	116~117 stations	5 min
Little Washita Watershed Micronet	Surface soil moisture content (0–5 cm layer, m <sup>3</sup> m <sup>-3</sup> )	9 stations	hourly

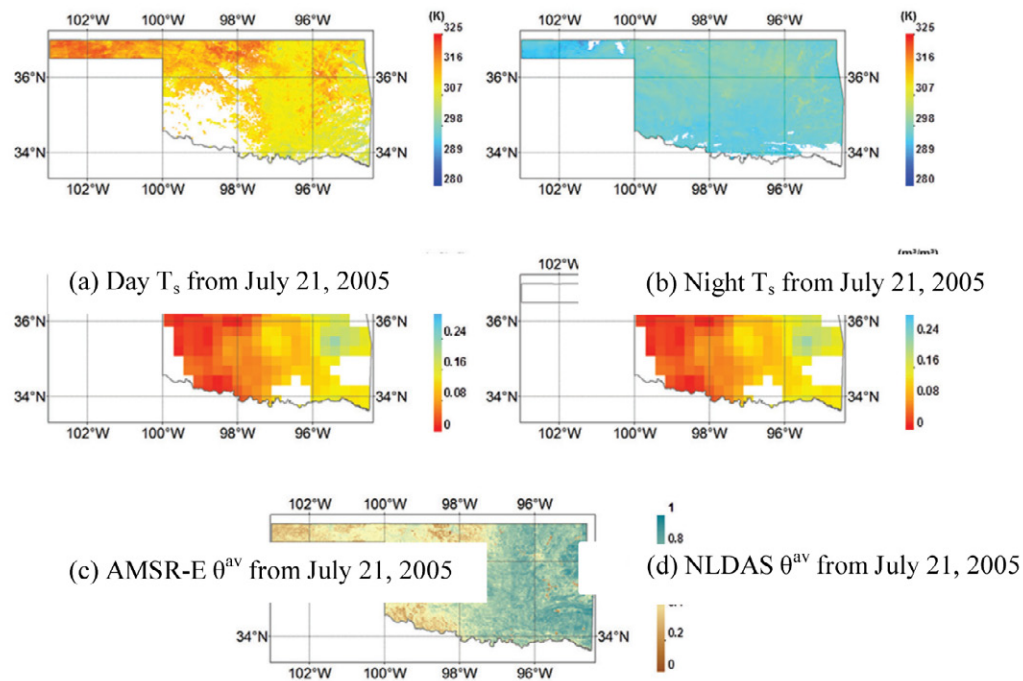


Fig. 2. Maps of variables used in the soil moisture downscaling algorithm from 21 July 2005 over Oklahoma, MODIS Aqua 1-km land surface temperature (a) during the day and (b) at night; (c) 1/4° spatial resolution AMSR-E soil moisture; (d) 1/8° spatial resolution NLDAS soil moisture; (e) MODIS Aqua 1-km NDVI.

parameters for hydrological studies from 2002 to 2011 (Njoku et al., 2003; Njoku and Chan, 2006). The soil moisture retrievals from AMSR-E are posted on 1/4° (25 km) spatial resolution. The estimate of AMSR-E soil moisture accuracy is approximately 0.1 m<sup>3</sup> m<sup>-3</sup> and cannot be estimated in areas where vegetation biomass exceeds 1.5 kg m<sup>-2</sup> (Njoku and Li, 1999).

The AMSR-E soil moisture was estimated using the single channel algorithm (Jackson, 1993; Jackson et al., 2010). The single channel algorithm uses the X-band observations at H-polarization (the most sensitive channel) for estimation of soil moisture. The C-band observations cannot be used for land surface applications because they are significantly affected by radio frequency interference. The land surface temperature was estimated using the 37-GHz v-pol observations. The AVHRR derived climatological dataset was used

to account for vegetation impact on microwave radiations emitted from the soil surface. For matching with other georeferenced datasets, a drop-in-the-bucket method was applied to the AMSR-E data, and it was gridded to a 25- by 25-km Equal-Area Scalable Earth (EASE) grid cell size. This method averaged all the AMSR-E points by determining if their center coordinates were within the border of a particular EASE grid cell.

### MODIS Data

Surface temperature data corresponded to the Oklahoma local times of 01:30 and 13:30, as well as the NDVI from MODIS/Aqua. MODIS has 36 spectral bands, including visible, near-infrared, and thermal infrared spectrums, and provides 44 global data products (Justice et al., 2002). The algorithms to derive the MODIS products are well established and have been extensively

evaluated, including NDVI (Tucker, 1979; Myneni et al., 1995), leaf area index (Myneni et al., 2002), land cover classification (DeFries et al., 1998; Friedl et al., 2002), and surface temperature (Wan and Li, 1997). In the current study, surface temperature and NDVI products at two different spatial resolutions were used for downscaling soil moisture. The datasets included 1-km daily surface temperature (MYD11A1), 1-km biweekly NDVI (MYD13A2), and 500-m biweekly Climate Modeling Grid (CMG) NDVI (MYD13C1). The dry down lines of soil moisture during May 2004, July 2005, and August 2005 in Oklahoma were examined. During these 3 mo, clear days (due to the requirement of surface temperature in our algorithm) were selected for the downscaling algorithm application.

### AVHRR Data

Before the launch of the Aqua satellite and the availability of MODIS data, the 5-km CMG daily NDVI data from AVHRR sensor (AVH13C1) was used. The AVHRR sensor is on board the NOAA satellites, including N07, N09, N11, and N14, and provides global and long-term surface ground measurements. Daily AVHRR NDVI data are available between 1981 and 1999 (Land Long Term Data Record, 2011). Because the N14 orbit drifted greatly and degraded the data quality, AVHRR NDVI data after year 2000 was not used in this soil moisture downscaling curve fitting.

### Oklahoma Mesonet

The Oklahoma Mesonet is a network of 120 automated environmental monitoring stations with at least one site in each of the 77 counties in Oklahoma (McPherson et al., 2007). Environmental variables are obtained at intervals spanning every 5 to 30 min, depending on the variable. The data quality is verified by a series of automated and manual checks, performed by the Oklahoma Climatological Survey (Illston et al., 2008). In this investigation, 5-cm soil moisture content measurements from 116 stations were extracted and geolocated for comparison with the 1-km downscaled AMSR-E and NLDAS soil moisture values. The locations of the Oklahoma Mesonet stations are denoted by open yellow circles in Fig. 1.

### Little Washita Watershed Micronet

The Little Washita Watershed is located in the southwestern portion of Oklahoma and includes more than 20 stations within a 25- by 25-km region referred to as the Little Washita Micronet. The point watershed soil moisture observations from nine stations with the closest time to the Aqua overpass times: 1:30 and 13:30 were extracted and then averaged to match up with the estimated average daily soil moisture (Cosh et al., 2004; Jackson et al., 2010). The locations of these stations are denoted by red dots in Fig. 1.

## Methodology

### Daily NDVI Interpolation

The AVHRR and MODIS NDVI products at spatial resolutions of 5- and 1-km were used for model building and implementation. The biweekly 5-km MODIS NDVI, between 2003 and 2011, was aggregated to 12.5 km and geolocated to NLDAS pixels for gap filling the AVHRR NDVI data. The biweekly 1-km MODIS NDVI between 2003 and 2011 was input to the model for retrieving 1-km soil moisture. To provide 5- and 1-km resolution NDVI estimates on a daily basis, all the NDVI records through each year of 2003 through 2011 were fitted using the sinusoidal method as

$$\text{NDVI}_d = a_0 \sin(a_1 D + a_2) + a_3 \quad [1]$$

where  $a_0$ ,  $a_1$ ,  $a_2$ , and  $a_3$  are the regression coefficients;  $\text{NDVI}_d$  is the daily NDVI value; and  $D$  is the day of year. This equation was applied to the biweekly NDVI data, for all years, to obtain daily NDVI values. This method assumes a single crop cycle and has to be modified for locations with multiple crop cycles. So the daily NDVI varies in a near sinusoidal fashion through all the days every year (Zhang et al., 2003; Knight et al., 2006). Almost the entire study domain is dominated by forest, rangeland, or winter wheat (*Triticum aestivum* L.) (single crop cycle).

### Thermal Inertia Theory

Thermal inertia is the resistance of a material to temperature change, which is indicated by time dependent variations in temperature during a full heating/cooling cycle. It is defined as the square root of the product of the material's bulk thermal conductivity ( $k$ ) and volumetric heat capacity, where the latter is the product of density ( $\rho$ ) and specific heat capacity ( $c$ ):

$$I = \sqrt{k\rho c} \quad [2]$$

An approximation to thermal inertia can be obtained from the amplitude of the diurnal temperature curve. The temperature of a material with low thermal inertia will change more during the day than a material with high thermal inertia. Many attempts have been made since the Heat Capacity Mapping Mission (NSSDC ID: 1978-041A-01; NASA, 2011), the first of a series of Applications Explorer Missions (Heilman and Moore, 1982), to capture the thermal characteristics of the earth surface. The objective of the Heat Capacity Mapping Mission was to provide comprehensive, accurate, high-spatial-resolution thermal surveys of the surface of the earth to determine thermal inertia.

The heat capacity of water is greater than dry soil. Therefore, soil with higher moisture content corresponds to smaller temperature changes. Because soil volumetric heat capacity increases with higher soil moisture, it is our assertion that lower daily average soil moisture ( $\theta^{\text{av}}$ ) will correspond to higher daily temperature

differences ( $\Delta T_s$ ) and vice-versa. Higher soil moisture also corresponds to higher evapotranspiration, cooling the soil surface.  $\Delta T_s$  can be described as

$$\Delta T_s = T_{\max} - T_{\min} \quad [3]$$

where  $T_{\max}$  and  $T_{\min}$  are the daily highest and lowest temperatures, respectively. The two local overpass times of MODIS/Aqua approximately correspond to the highest and lowest temperatures.

### Construction of the Downscaling Model

The MODIS sensor provides two very important products: NDVI and surface temperature  $T_s$ . In this study, these two variables were extracted for each 1-km MODIS pixel ( $i, j$ ) in the  $1/4^\circ$  gridded AMSR-E radiometer data. We denote these variables by NDVI ( $i, j$ ) and  $T_s(i, j)$ , respectively. The AMSR-E derived soil moisture, corresponding to the 01:30 (descending orbit) overpass, is denoted as  $\Theta^a$  while 13:30 (ascending orbit) overpass is denoted as  $\Theta^p$  for the entire  $1/4^\circ$  pixel. Soil moisture values for AM and the PM overpass for each of the MODIS pixels are referred as  $\theta^a(i, j)$  and  $\theta^p(i, j)$ , respectively. The time-average value of the pixel soil moisture is denoted as  $\theta^{av}(i, j)$ , which refers to the predicted arithmetic mean of soil moisture for the 1-km MODIS pixel of the AM and PM overpass (see Fig. 3). The MODIS sensor on Aqua was used because it matched the time of AMSR-E soil moisture estimates.

Three principles motivate the pixel-based downscaling algorithm. First, we must consider that the soil moisture history of each pixel is unique with regard to precipitation, evapotranspiration, and runoff and can be summarized by the average soil moisture  $\theta^{av}(i, j)$ . Second, based on the thermal inertia theory, the thermal inertia

and soil moisture depend on soil thermal conductivity, which for a wet pixel will show a smaller change and for a dry pixel will show a larger change in surface temperature (Minacapilli et al., 2009) due to modulation by evapotranspiration. Wetter pixels have larger evapotranspiration and lower surface temperature change and vice-versa (Kurc and Small, 2004). Third, vegetation biomass within each pixel will vary and can also modulate the change of surface temperature, which is represented by  $\Delta T_s$  (Merlin et al., 2010; Lakshmi et al., 2011). The comparison of the pixel sizes between the three datasets and the regression curve building method is shown in Fig. 3.

The key to the proposed disaggregation procedure is establishing the relationship between the change in surface temperature and the average soil moisture for the 1-km pixel. To construct the regression relationship, we plotted separately the daily NLDAS from all the years of a particular month of the study period (i.e., the July plot will have data for the surface temperature change and the average NLDAS soil moisture for all years from 1981 to 2011). The data for equal NDVI lines at increments of 0.3 in NDVI were subsequently organized. For example, during some months (e.g., January), vegetation growth was limited and few NDVI lines in the upper Midwest might be constructed. On the other hand, during other periods, such as July in the upper Midwest, rapid changes in NDVI due to crop growth could occur and many NDVI lines would be created. The daily NLDAS lines based on temperature difference and averaged soil moisture at 01:30 and 13:30 of all the days from 1981 to 2011 (except 2000–2002) were then fitted.

For simplicity, a linear regression model between the daily average soil moisture  $\theta^{av}(s, t)$  and daily temperature difference  $\Delta T_s(s, t)$  at NLDAS scale for each month was developed as follows

$$\theta^{av}(s, t) = a_0 + a_1 \Delta T_s(s, t) \quad [4]$$

where  $s$  and  $t$  represent the NLDAS pixel location,  $a_0$  and  $a_1$  are the regression model coefficients that correspond to several different NDVI intervals. The growing season between May and September was examined in this study, and the NDVI was subdivided into three intervals: 0–0.3, 0.3–0.6, and 0.6–1. For each month, three NLDAS-based regression lines of each pixel, corresponding to the three NDVI intervals, were built and the regression coefficients were obtained.

### Correction of 1-km Downscaled Soil Moisture

We presumed that the soil moisture variation within each NLDAS pixel could be ignored and the downscaling model at  $1/8^\circ$  could be applied to the 1-km MODIS surface temperature. On a daily basis, we used the lines corresponding to the NLDAS data closest to the MODIS pixel to calculate the 1-km averaged soil moisture  $\theta^{av}(i, j)$  from the  $\Delta T_s(i, j)$  of each 1-km MODIS pixel by Eq. [4]. We then averaged  $\theta^{av}(i, j)$  from all the 1-km MODIS pixels and compared the values to daily average AMSR-E soil moisture  $(\Theta^a + \Theta^p)/2$ ,

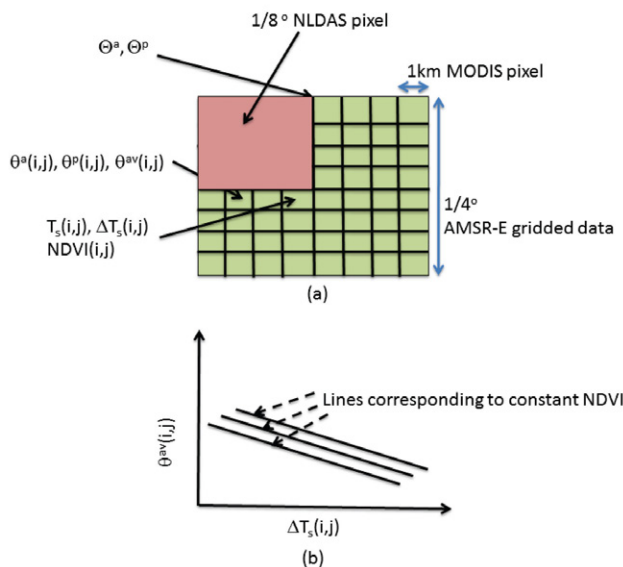


Fig. 3. (a) The various elements in the disaggregation procedure and (b) construction of the lines corresponding to constant NDVI between average soil moisture and change in surface temperature.

and then corrected each  $\theta^{av}(i,j)$  with the difference between  $(\Theta^a + \Theta^p)/2$  and averaged  $\theta^{av}(i,j)$  within the AMSR-E pixel. The cloud-covered or data gap pixels of MODIS and AMSR-E were not used in the calculation. The corrected soil moisture  $\theta^{avc}(i,j)$  is given by

$$\theta^{avc}(i,j) = \theta^{av}(i,j) + \left[ \left( \frac{\Theta^a + \Theta^p}{2} \right) - \frac{1}{N} \sum_{i,j} \theta^{av}(i,j) \right] \quad [5]$$

where  $N$  is the number of 1-km  $\theta^{av}(i,j)$  within the AMSR-E pixel. We subsequently generated daily values of  $\theta^{avc}(i,j)$  at 1 km. This satisfied the following conditions: (i) the average of the disaggregated soil moistures over the AMSR-E pixel is the same as that recorded by AMSR-E; (ii) the MODIS 1-km vegetation modulates the distribution of the disaggregated soil moisture through its relationship with the daily change in the MODIS 1-km surface temperature; and (iii) the 1-km scale changes in surface temperature is reflected in the soil moisture distribution as evidenced in the disaggregated soil moisture. The limitation of this methodology is that it can only be applied over areas with no cloud cover. The data flow diagram for this algorithm is shown in Fig. 4.

## Results

### $\theta^{av} - \Delta T_s$ Regression Lines

Figure 5 shows the regression fit results between NLDAS derived daily temperature difference and daily average soil moisture of a pixel (101.875~102°W, 35.125~35.625°N) for the growing months of May, July, and August. Notice that the daily average soil moisture values for all the months generally range between 0.05 and 0.3 m<sup>3</sup> m<sup>-3</sup>. The points that correspond to each NDVI interval (0–0.3, 0.3–0.6, and 0.6–1.0) yield nearly parallel lines

( $R^2$  values for July are 0.54, 0.56, and 0.40, respectively, for each NDVI interval). The relationship between daily temperature difference ( $\Delta T_s$ ) and daily average soil moisture ( $\theta^{av}$ ) of the particular NLDAS pixel (Fig. 5) of different NDVI intervals was also examined by Student's  $t$  test. The results show that the relationships for May 2004, July 2005, or August 2005 at  $\alpha = 0.05$  level are statistically significant through all three NDVI intervals. Further, the daily average soil moisture has a negative relationship with the daily temperature change, which is consistent with the assumptions that (i) the temperature change between morning and night is determined by pixel wetness and (ii) vegetation modulates the change of surface temperature and the pixel with higher vegetation is less sensitive to the temperature change.

### 1-km Downscaled Soil Moisture Analysis

Examples of maps of daily 1-km downscaled soil moisture are shown for 22 May 2004, 17 July 2005, and 9 Aug. 2005 (Fig. 6). The 1-km downscaled soil moistures in the lower Midwest part of Oklahoma (Fig. 6iii, vi, and ix) were missing because precipitation and heavy cloud cover dominated this area, resulting in missing MODIS surface temperature data. This area also corresponded to a gap between AMSR-E sensor swaths. These downscaled maps illustrate the pattern of soil moisture distribution where soil moisture content gradually increases from west to east, which corresponds to the NDVI variation in Oklahoma. In addition, the 1-km downscaled soil moisture maps also exhibit similar spatial patterns as those of AMSR-E and NLDAS.

The NLDAS soil moisture (Fig. 6i, iv, and vii), which is obtained from models, always has complete coverage because it is not impacted by cloud cover or missing data due to gaps in swath

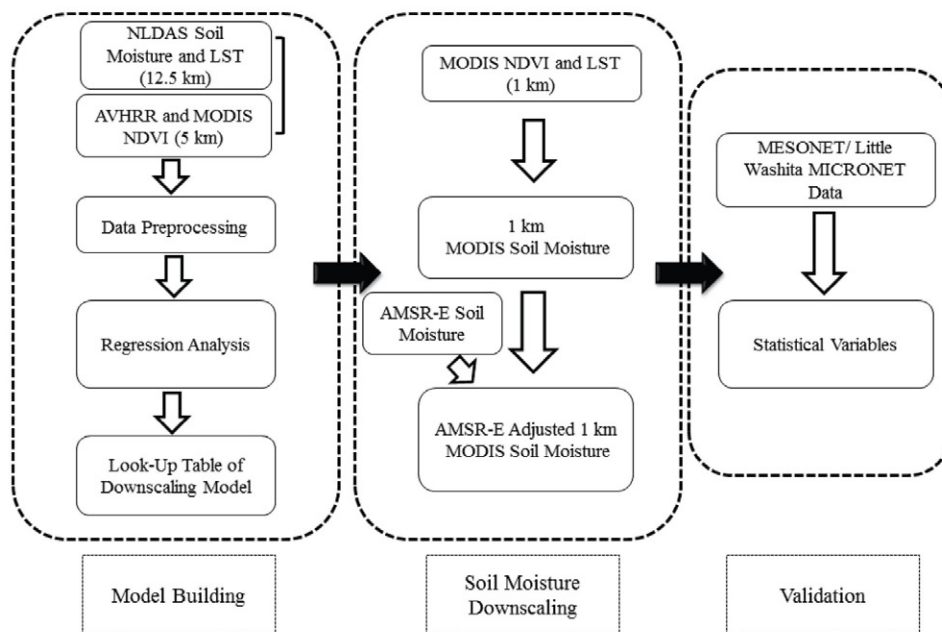


Fig. 4. Data flow of the soil moisture downscaling algorithm

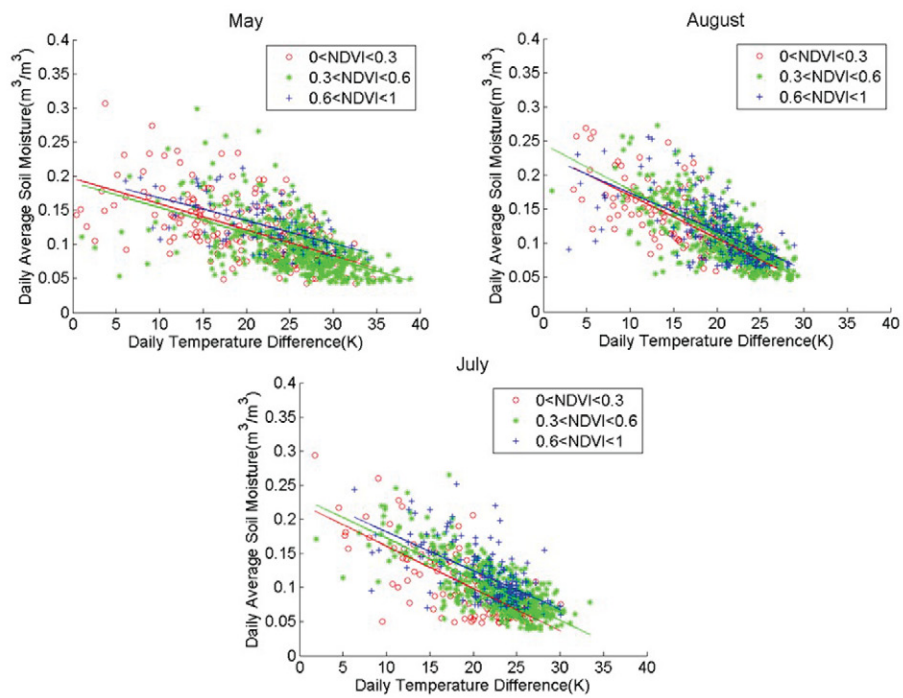


Fig. 5. Daily temperature difference versus daily average soil moisture corresponding to (101.875~102°W, 35.125~35.625°N) and different NDVI values for May, August, and July.

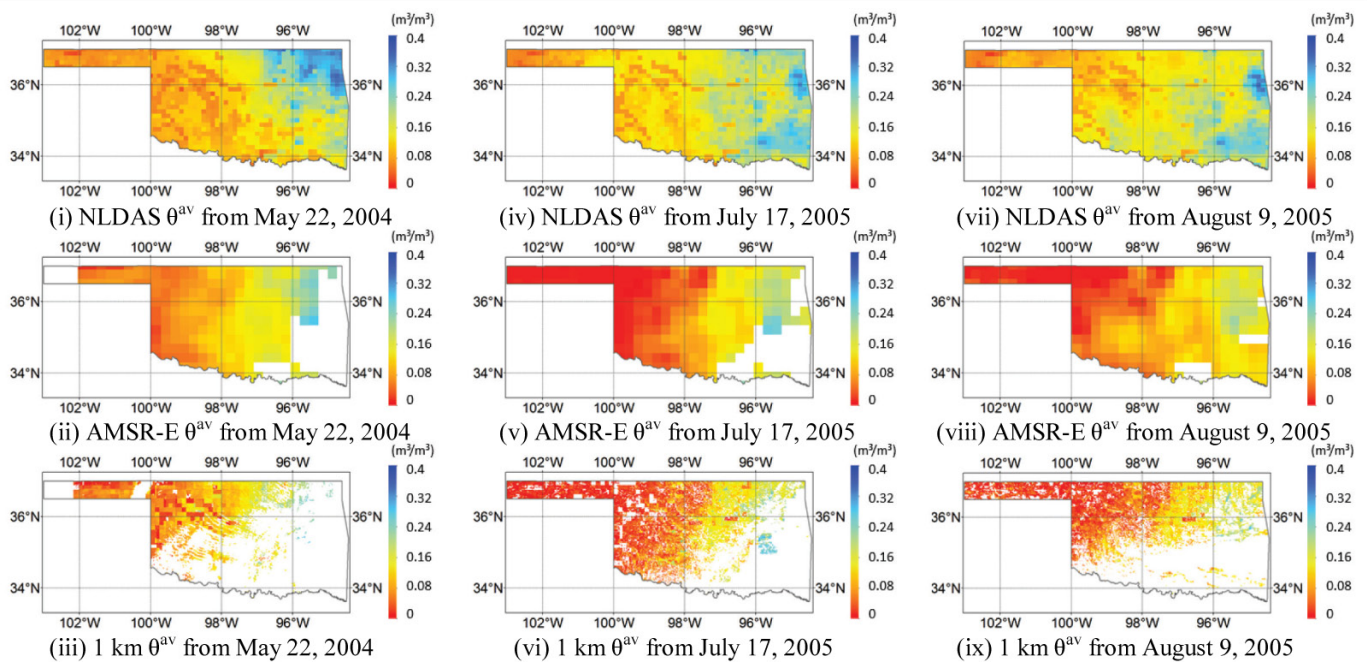


Fig. 6. Maps of the NLDAS, AMSR-E, and 1-km soil moisture ( $\text{m}^3 \text{m}^{-3}$ ) from May 22, 2004, July 17, 2005 and August 9, 2005 in Oklahoma.

coverage. On 22 May 2004 (Fig. 6i–iii), a wet area in the northeast corner of Oklahoma was not clearly shown by either the AMSR-E or the 1-km downscaled soil moisture. In general the spatial patterns of the three estimates for the 22 May 2004 case resemble each other. On 17 July 2005, the western half of Oklahoma was very dry with soil moisture close to  $0.02 \text{ m}^3 \text{ m}^{-3}$  and with larger

values in the east. The spatial structure shown by the 1-km soil moisture demonstrated variability in the dry western part of the state, which was not observable using the  $1/4^\circ$  AMSR-E estimates alone. In addition, the 1-km soil moisture captured the wet area in the east central part of the state. A similar west-to-east dry-to-wet

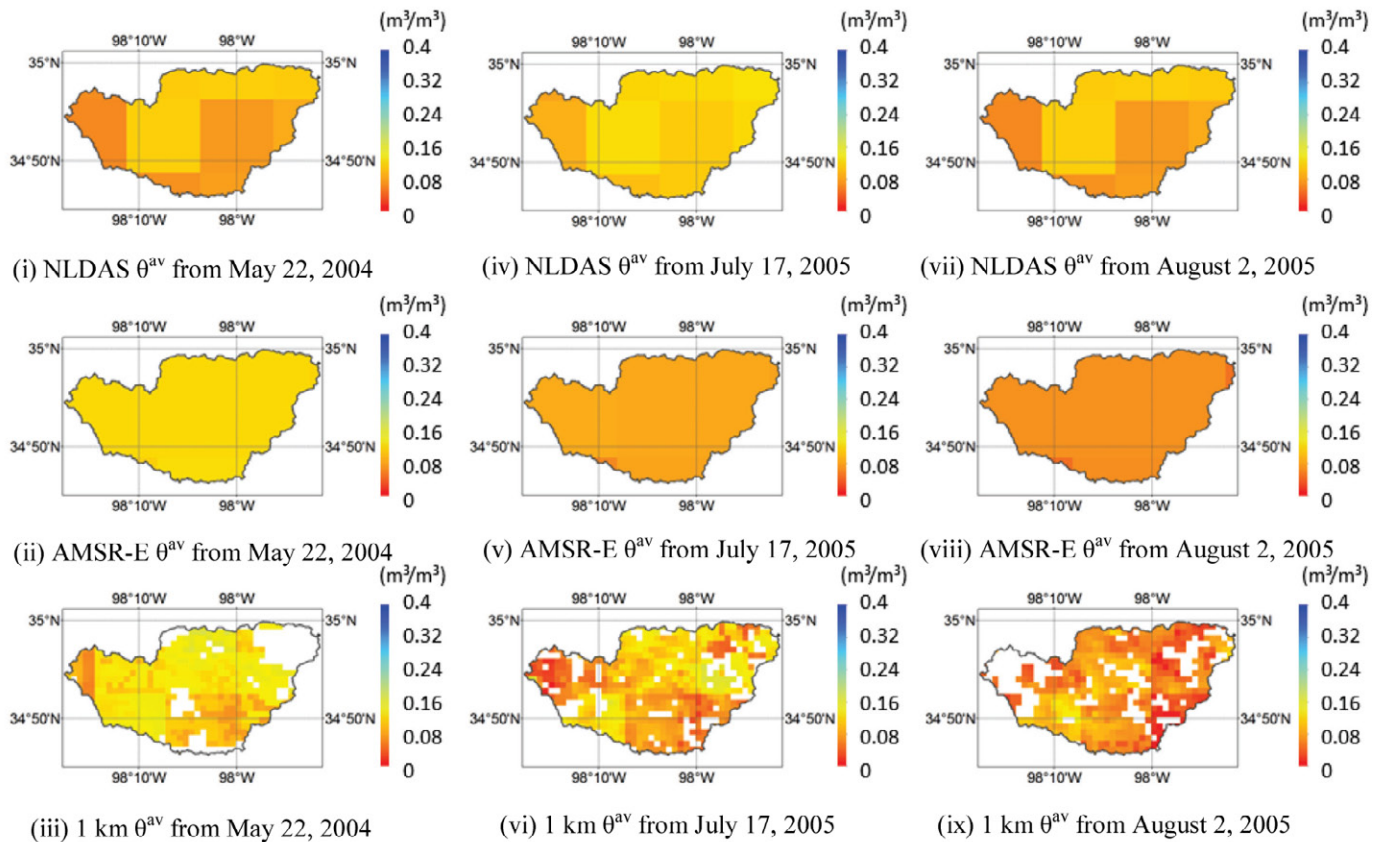


Fig. 7. Maps of the NLDAS, AMSR-E, and 1-km soil moisture ( $\text{m}^3 \text{m}^{-3}$ ) from 22 May 2004, 17 July 2005, and 2 August 2005 in Little Washita.

pattern could be observed in all the estimates of the soil moisture for 9 August 2005.

Focusing on the Little Washita region (Fig. 7), the spatial distribution of soil moisture exhibited greater heterogeneity in 1-km downscaled map, depicting far more dry 1-km pixels than shown in the AMSR-E and NLDAS maps, easily explainable by single AMSR-E pixel that covers the entire watershed and the few ( $\sim 5$ ) NLDAS pixels. The ability to show heterogeneity in soil moisture at the catchment scale is one of the strong points of the 1-km downscaled soil moisture product. This is seen especially in a time series of soil moisture changes in 1-km downscaled map of the Little Washita watershed during July 2005 (Fig. 8). Here, the soil moisture dry down can be clearly observed through these days, particularly in the westernmost portion of the watershed, as well as a smaller subcatchment near the middle-east portion of the larger watershed.

### Validation by Oklahoma Mesonet Soil Moisture Data

Validating the disaggregation algorithm was done by comparing two sets of ground observations—Oklahoma Mesonet and Little Washita watershed soil moisture values—with the three gridded soil moisture datasets—NLDAS, AMSR-E, and 1-km

disaggregated soil moisture. The ground observation soil moisture points were compared with closest pixel of the three gridded soil moisture datasets. We set a threshold for the minimum number of ground observation points to compare with the three gridded soil moisture datasets from the Mesonet and Little Washita watershed (20 points and 5 points, respectively). Because the NLDAS uses Oklahoma Mesonet soil moisture (Luo et al., 2003) and has been scaled to Mesonet data, the NLDAS soil moisture should perform better than the AMSR-E and 1-km estimates.

The statistical variables being validated include slope, RMSE, unbiased RMSE, and spatial SD. The equations are as follows:

$$m = \frac{\hat{\theta}_i}{\theta_i}$$

$$\text{RMSE} = \sqrt{\frac{\sum_{i=1}^n (\hat{\theta}_i - \theta_i)^2}{n}}$$

$$\text{RMSE}^* = \sqrt{\frac{\sum_{i=1}^n (\hat{\theta}_i^* - \theta_i)^2}{n}}$$

$$\sigma = \sqrt{\frac{\sum_{i=1}^n (\hat{\theta}_i - \bar{\theta})^2}{n}}$$

where  $m$  is the slope of linear regression between estimated soil moisture  $\hat{\theta}$  (1 km, AMSR-E and NLDAS) and in situ soil moisture  $\theta$  (Mesonet and Micronet).  $RMSE^*$  is the unbiased RMSE.  $\hat{\theta}_i^*$  is the predicted soil moisture value from linear regression between estimated soil moisture  $\hat{\theta}$  and in situ soil moisture  $\theta$ ,  $\sigma$  is the spatial standard deviation of each soil moisture data, including estimated soil moisture and in situ soil moisture,  $n$  is the number of data points over the study area (Mesonet or Micronet) collected in a single day. The  $RMSE$  and  $RMSE^*$  are used to characterize the uncertainty of estimated soil moisture  $\hat{\theta}$  to in situ soil moisture  $\theta$ . The spatial standard deviation  $\sigma$  is used to represent the spatial variation of the study area. The Chi-squared test was also applied for both Mesonet and Micronet comparisons for examining the goodness of fit, which is specified at  $\alpha = 0.05$  level.

Table 3 shows the statistical values of comparisons with Mesonet data for single days during May 2004, July 2005, and August 2005, while Table 4 shows the monthly overall and total averaged values of the 3 mo. From Table 3, we note that the slope of 1-km downscaled comparison is generally better than NLDAS and AMSR-E, while the unbiased RMSE and spatial standard deviation of some days are better as well. The  $p$  value of Chi-squared test (at  $\alpha = 0.05$  level) of 1-km downscaled soil moisture is statistically better than NLDAS and AMSR-E. Table 3 also shows the day-to-day variability of the performance of the 1-km soil moisture estimates as compared to AMSR-E and NLDAS, as well as the changes in the spatial standard deviation as compared to the Mesonet estimates.

From Table 4, we observed that the slope of 1-km downscaled comparison for 2 mo (July 2005 and August 2005), which are 0.078 and 0.2  $m^3 m^{-3}$ , respectively, is better than NLDAS and AMSR-E, and the total averaged slope of 1-km downscaled comparison as well. Although the RMSE of 1-km downscaled comparison is worse than NLDAS and AMSR-E, the unbiased RMSE of 1-km downscaled comparison for all 3 mo and overall is very similar to NLDAS and AMSR-E (0.042  $m^3 m^{-3}$  versus 0.04 and 0.042  $m^3 m^{-3}$ , respectively). In addition, the spatial standard deviation of 1-km downscaled results on May 2004 and August 2005, which is 0.058 and 0.044  $m^3 m^{-3}$ , respectively, are closer to Mesonet than NLDAS, which is 0.066 and 0.047  $m^3 m^{-3}$  and a little further than AMSR-E, which is 0.056 and 0.047  $m^3 m^{-3}$ . These results demonstrate that the disaggregated soil moisture provides improvements in both accuracy and spatial resolution.

We also note that the soil moisture values for all three datasets are systematically lower than the in situ Mesonet observation values. This could be attributed to several factors. First, the accuracy of AMSR-E soil moisture is limited. This methodology

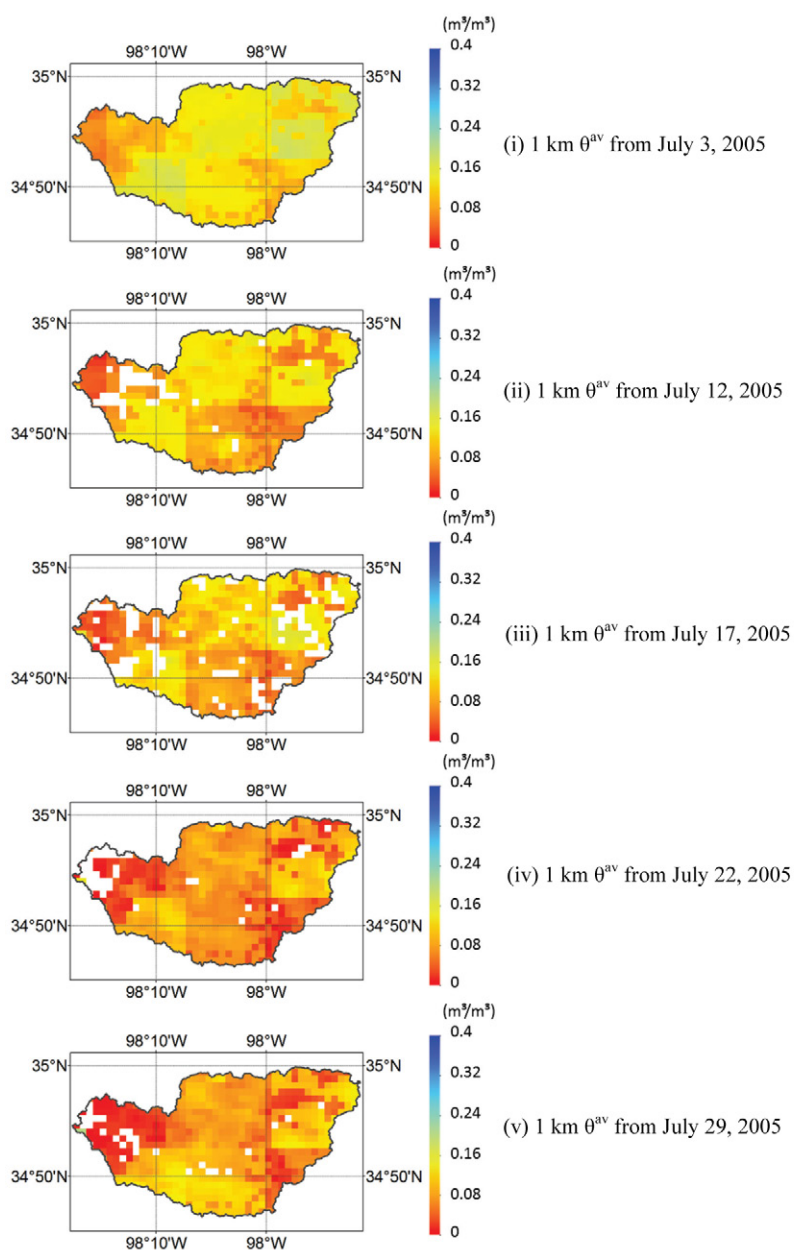


Fig. 8. (i–v) Time-series maps of 1-km soil moisture ( $m^3 m^{-3}$ ) of 5 d on July 2005 show the dry-down tendency in Little Washita region.

is based on preserving the 25-km mean soil moisture from the AMSR-E platform. So, any overall day-to-day bias presented in the AMSR-E soil moisture retrievals will appear in the disaggregated 1-km estimates. Second, the MODIS retrieved daytime surface temperature is higher than the NLDAS land surface model output, particularly during the growing season. This may cause the daily temperature difference to be greater than NLDAS and consequently the downscaled soil moisture would be lower than NLDAS. Third, the Oklahoma Mesonet is equipped with sensors to measure soil water potential (model 229-L, Campbell Scientific), which is then converted to volumetric soil moisture. Biases in this conversion may be present in gravimetric and neutron

Table 3. Comparison statistics between the 1-km downscaled, NLDAS and AMSR-E soil moisture compared to the Oklahoma Mesonet for 3 mo. The 1-km downscaled values are underlined.

Day	Dataset	Slope	RMSE	m <sup>3</sup> m <sup>-3</sup>		p value	Number of points
				Unbiased RMSE	Spatial SD		
2 May 2004	1-km downscaled	<u>0.404</u>	<u>0.136</u>	<u>0.063</u>	<u>0.074</u>	<u>0.019</u>	81
	AMSR-E	0.442	0.132	0.061	0.07	0.024	
	NLDAS	0.552	0.101	0.056	0.071	0.132	
	Mesonet				0.067		
4 May 2004	1-km downscaled	<u>0.268</u>	<u>0.144</u>	<u>0.057</u>	<u>0.069</u>	<u>0.009</u>	81
	AMSR-E	0.35	0.141	0.055	0.065	0.009	
	NLDAS	0.497	0.108	0.052	0.069	0.1	
	Mesonet				0.058		
6 May 2004	1-km downscaled	<u>-0.285</u>	<u>0.138</u>	<u>0.032</u>	<u>0.031</u>	<u>0.005</u>	87
	AMSR-E	-0.341	0.135	0.033	0.026	0.006	
	NLDAS	-0.579	0.108	0.033	0.027	0.063	
	Mesonet				0.034		
7 May 2004	1-km downscaled	<u>0.37</u>	<u>0.151</u>	<u>0.053</u>	<u>0.056</u>	<u>0.006</u>	35
	AMSR-E	0.395	0.146	0.051	0.052	0.01	
	NLDAS	0.423	0.118	0.048	0.073	0.073	
	Mesonet				0.055		
8 May 2004	1-km downscaled	<u>0.241</u>	<u>0.108</u>	<u>0.032</u>	<u>0.057</u>	<u>0.167</u>	45
	AMSR-E	0.263	0.109	0.032	0.052	0.165	
	NLDAS	0.703	0.086	0.031	0.046	0.378	
	Mesonet				0.033		
9 May 2004	1-km downscaled	<u>0.544</u>	<u>0.119</u>	<u>0.050</u>	<u>0.041</u>	<u>0.176</u>	24
	AMSR-E	0.72	0.116	0.049	0.041	0.192	
	NLDAS	1.071	0.096	0.043	0.072	0.322	
	Mesonet				0.052		
20 May 2004	1-km downscaled	<u>0.462</u>	<u>0.105</u>	<u>0.064</u>	<u>0.062</u>	<u>0.146</u>	57
	AMSR-E	0.453	0.101	0.061	0.06	0.148	
	NLDAS	0.717	0.109	0.06	0.08	0.103	
	Mesonet				0.072		
22 May 2004	1-km downscaled	<u>0.884</u>	<u>0.128</u>	<u>0.025</u>	<u>0.1</u>	<u>0.027</u>	34
	AMSR-E	0.993	0.122	0.028	0.113	0.041	
	NLDAS	1.501	0.111	0.016	0.101	0.086	
	Mesonet				0.062		
23 May 2004	1-km downscaled	<u>1.04</u>	<u>0.11</u>	<u>0.054</u>	<u>0.063</u>	<u>0.038</u>	60
	AMSR-E	0.496	0.11	0.052	0.056	0.028	
	NLDAS	-0.01	0.107	0.049	0.075	0.048	
	Mesonet				0.06		
30 May 2004	1-km downscaled	<u>-0.012</u>	<u>0.118</u>	<u>0.023</u>	<u>0.043</u>	<u>0.107</u>	37
	AMSR-E	0.112	0.114	0.022	0.043	0.109	
	NLDAS	0.14	0.122	0.018	0.056	0.049	
	Mesonet				0.029		
31 May 2004	1-km downscaled	<u>0.25</u>	<u>0.105</u>	<u>0.041</u>	<u>0.043</u>	<u>0.073</u>	65
	AMSR-E	0.254	0.099	0.039	0.039	0.095	
	NLDAS	0.488	0.106	0.037	0.053	0.086	
	Mesonet				0.042		

Table 3. Continued.

Day	Dataset	Slope	RMSE	Unbiased RMSE	Spatial SD	<i>p</i> value	Number of points
			$\text{m}^3 \text{m}^{-3}$				
3 July 2005	1-km downscaled	<u>0.237</u>	<u>0.166</u>	<u>0.059</u>	<u>0.055</u>	<u>0.002</u>	85
	AMSR-E	0.039	0.161	0.064	0.034	0.007	
	NLDAS	0.095	0.119	0.063	0.025	0.117	
	Mesonet				0.064		
8 July 2005	1-km downscaled	<u>0.224</u>	<u>0.177</u>	<u>0.047</u>	<u>0.061</u>	<u>0.002</u>	85
	AMSR-E	0.08	0.169	0.048	0.052	0.005	
	NLDAS	0.168	0.106	0.047	0.045	0.224	
	Mesonet				0.048		
10 July 2005	1-km downscaled	<u>-0.043</u>	<u>0.174</u>	<u>0.053</u>	<u>0.06</u>	<u>0.001</u>	83
	AMSR-E	-0.005	0.162	0.053	0.052	0.004	
	NLDAS	0.213	0.113	0.051	0.048	0.127	
	Mesonet				0.053		
12 July 2005	1-km downscaled	<u>0.032</u>	<u>0.162</u>	<u>0.047</u>	<u>0.059</u>	<u>0.003</u>	90
	AMSR-E	-0.007	0.154	0.047	0.052	0.008	
	NLDAS	-0.013	0.091	0.047	0.046	0.361	
	Mesonet				0.047		
17 July 2005	1-km downscaled	<u>0.176</u>	<u>0.168</u>	<u>0.043</u>	<u>0.057</u>	-	95
	AMSR-E	0.228	0.165	0.043	0.052	-	
	NLDAS	0.16	0.104	0.043	0.045	0.145	
	Mesonet				0.043		
21 July 2005	1-km downscaled	<u>-0.262</u>	<u>0.13</u>	<u>0.031</u>	<u>0.047</u>	<u>0.009</u>	99
	AMSR-E	-0.141	0.125	0.031	0.05	0.014	
	NLDAS	-0.106	0.09	0.031	0.047	0.215	
	Mesonet				0.031		
22 July 2005	1-km downscaled	<u>-0.146</u>	<u>0.16</u>	<u>0.035</u>	<u>0.051</u>	-	102
	AMSR-E	-0.027	0.153	0.035	0.05	-	
	NLDAS	-0.108	0.112	0.035	0.046	0.059	
	Mesonet				0.035		
28 July 2005	1-km downscaled	<u>0.345</u>	<u>0.146</u>	<u>0.043</u>	<u>0.076</u>	<u>0.01</u>	103
	AMSR-E	0.305	0.137	0.044	0.058	0.017	
	NLDAS	0.217	0.098	0.044	0.047	0.209	
	Mesonet				0.045		
29 July 2005	1-km downscaled	<u>0.295</u>	<u>0.166</u>	<u>0.039</u>	<u>0.073</u>	-	79
	AMSR-E	0.16	0.159	0.039	0.047	-	
	NLDAS	0.098	0.119	0.039	0.034	0.031	
	Mesonet				0.039		
31 July 2005	1-km downscaled	<u>-0.077</u>	<u>0.155</u>	<u>0.032</u>	<u>0.051</u>	-	106
	AMSR-E	-0.067	0.145	0.032	0.056	-	
	NLDAS	-0.255	0.111	0.032	0.048	0.036	
	Mesonet				0.032		
2 Aug. 2005	1-km downscaled	<u>0.056</u>	<u>0.164</u>	<u>0.036</u>	<u>0.036</u>	-	80
	AMSR-E	0.077	0.16	0.036	0.051	-	
	NLDAS	-0.307	0.124	0.035	0.051	0.015	
	Mesonet				0.053		
4 Aug. 2005	1-km downscaled	<u>-0.346</u>	<u>0.143</u>	<u>0.025</u>	<u>0.026</u>	<u>0.045</u>	26

Table 3. Continued.

Day	Dataset	Slope	RMSE	Unbiased RMSE	Spatial SD	<i>p</i> value	Number of points
				$\text{m}^3 \text{m}^{-3}$			
	AMSR-E	-0.46	0.138	0.025	0.033	0.067	
	NLDAS	-1.17	0.106	0.023	0.035	0.427	
	Mesonet				0.059		
9 Aug. 2005	1-km downscaled	<u>0.119</u>	<u>0.167</u>	<u>0.041</u>	<u>0.041</u>	-	51
	AMSR-E	0.043	0.162	0.041	0.049	-	
	NLDAS	0.051	0.113	0.041	0.051	0.086	
	Mesonet				0.046		
24 Aug. 2005	1-km downscaled	<u>0.393</u>	<u>0.147</u>	<u>0.047</u>	<u>0.055</u>	<u>0.073</u>	34
	AMSR-E	0.315	0.144	0.047	0.05	0.085	
	NLDAS	0.316	0.064	0.047	0.047	0.751	
	Mesonet				0.034		
25 Aug. 2005	1-km downscaled	<u>0.377</u>	<u>0.118</u>	<u>0.05</u>	<u>0.065</u>	<u>0.235</u>	27
	AMSR-E	0.366	0.122	0.05	0.049	0.207	
	NLDAS	0.121	0.062	0.054	0.049	0.823	
	Mesonet				0.046		
30 Aug. 2005	1-km downscaled	<u>0.601</u>	<u>0.18</u>	<u>0.024</u>	<u>0.039</u>	<u>0.003</u>	44
	AMSR-E	0.38	0.173	0.025	0.052	0.003	
	NLDAS	0.666	0.105	0.024	0.05	0.367	
	Mesonet				0.051		

Table 4. Monthly generalized comparison statistics between the 1-km downscaled, NLDAS and AMSR-E soil moisture compared to the Oklahoma Mesonet for 3 mo. The 1-km downscaled values are underlined.

Day	Dataset	Slope	RMSE	Unbiased		Number of points
				RMSE	Spatial SD	
				$\text{m}^3 \text{m}^{-3}$		
May 2004	1-km downscaled	<u>0.379</u>	<u>0.124</u>	<u>0.045</u>	<u>0.058</u>	606
	AMSR-E	0.376	0.120	0.044	0.056	
	NLDAS	0.500	0.107	0.040	0.066	
	Mesonet				0.051	
July 2005	1-km downscaled	<u>0.078</u>	<u>0.160</u>	<u>0.043</u>	<u>0.052</u>	927
	AMSR-E	0.057	0.153	0.044	0.050	
	NLDAS	0.047	0.106	0.043	0.043	
	Mesonet				0.044	
August 2005	1-km downscaled	<u>0.200</u>	<u>0.153</u>	<u>0.037</u>	<u>0.044</u>	262
	AMSR-E	0.120	0.150	0.037	0.047	
	NLDAS	-0.054	0.096	0.037	0.047	
	Mesonet				0.045	
Total	1-km downscaled	<u>0.219</u>	<u>0.146</u>	<u>0.042</u>	<u>0.054</u>	1795
	AMSR-E	0.184	0.141	0.042	0.051	
	NLDAS	0.164	0.103	0.040	0.052	
	Mesonet				0.047	

probe samples, of which RMSE is between 0.006 and 0.052  $\text{m}^3 \text{m}^{-3}$  (Illston et al., 2008). From the matric potential values, soil

water content is calculated by the van Genuchten (1980) equation, using coefficients based on soil parameters collected at the time

of installation. In addition, Minet et al. (2012) used ground penetrating radar derived soil moisture to study the uncertainties of field scale variability of surface soil moisture and concluded that these arise from the errors introduced in mapping and interpolation, and model inadequacies.

It has been observed in the data series that this methodology can result in a biased high soil moisture estimate in the Mesonet, compared to other sampling methods. Mesoscale models typically also provide high soil moisture estimates due to their shortcomings in modeling soil water infiltration. Because of these independent deficiencies, both the Mesonet soil moisture and NLDAS soil moistures are biased wet. The soil moisture estimates were rescaled to remove the bias to mitigate the calibration bias between different soil moisture datasets.

### Validation Using Little Washita Watershed Soil Moisture Data

Figure 9a,b shows the overall soil moisture and detrended soil moisture comparisons of NLDAS, AMSR-E, and 1-km downscaled data, with Little Washita Micronet. Table 5 shows the statistical values comparing Micronet data for single days on May 2004 and July 2005, while Table 6 shows the monthly overall and total averaged results of the 2 mo (August 2005 did not have enough valid values, so it was dropped). From Table 5, the slope of the 1-km downscaled results is obviously better than NLDAS

and AMSR-E, while the unbiased RMSE of some days is better than either NLDAS or AMSR-E. In addition, when comparing the Mesonet data, the spatial standard deviation for 1 km is significantly improved and much closer to Micronet than NLDAS and AMSR-E. The results of Chi-squared test (at  $\alpha = 0.05$ ) of all three dataset are not as good as the Mesonet comparison. However, improvement of the  $p$  value of 1-km downscaled results can be noticed comparing with the other two soil moisture datasets.

From Table 6, the overall slope and spatial standard deviation for 1-km downscaled result are 0.242 and  $0.021 \text{ m}^3 \text{ m}^{-3}$ , respectively, which shows significant advantages compared to NLDAS (0.096 and  $0.007 \text{ m}^3 \text{ m}^{-3}$ , respectively) and AMSR-E (0.076 and  $0.005 \text{ m}^3 \text{ m}^{-3}$ , respectively). The overall spatial standard deviation of Micronet observations was found to be 0.028 and the 1-km spatial standard deviation is 0.021—much closer to the Micronet observations as compared to AMSR-E and NLDAS, with 0.005 and 0.007, respectively. This will be particularly important in small watershed studies when one pixel of NLDAS might cover an entire catchment and not provide information on spatial variability. In addition, the unbiased RMSE of 1-km downscaled result is also better than NLDAS. Results show that RMSE 0.024 versus 0.025 for NLDAS on May 2004, 0.027 versus 0.031 for NLDAS on July 2005, and 0.026 versus 0.028 for NLDAS of total average. By analyzing the comparison plots of spatial standard variation between estimated soil moisture and Mesonet in situ data (Fig. 10),

Table 5. Comparison statistics between the 1-km downscaled, NLDAS and AMSR-E soil moisture compared to the Little Washita soil moisture observations for 3 mo. The 1-km downscaled values are underlined.

Day	Dataset	Slope	— $\text{m}^3 \text{ m}^{-3}$ —				Number of points
			RMSE	Unbiased RMSE	Spatial SD	$p$ value	
4 May 2004	1-km downscaled	<u>0.083</u>	<u>0.044</u>	<u>0.043</u>	<u>0.015</u>	<u>0.882</u>	9
	AMSR-E	0.083	0.041	0.031	0.005	0.891	
	NLDAS	0.158	0.048	0.04	0.016	0.835	
	Micronet				0.044		
6 May 2004	1-km downscaled	<u>0.1</u>	<u>0.052</u>	<u>0.041</u>	<u>0.015</u>	<u>0.785</u>	9
	AMSR-E	0.1	0.041	0.026	0.006	0.863	
	NLDAS	0.173	0.058	0.036	0.014	0.729	
	Micronet				0.042		
8 May 2004	1-km downscaled	<u>0.346</u>	<u>0.077</u>	<u>0.017</u>	<u>0.012</u>	<u>0.662</u>	9
	AMSR-E	0.165	0.069	0.009	0.004	0.686	
	NLDAS	0.145	0.078	0.022	0.011	0.660	
	Micronet				0.023		
15 May 2004	1-km downscaled	<u>0.149</u>	<u>0.037</u>	<u>0.017</u>	<u>0.01</u>	<u>0.889</u>	9
	AMSR-E	–	0.05	0.036	0.004	0.810	
	NLDAS	0.065	0.035	0.033	0.01	0.912	
	Micronet				0.036		
22 May 2004	1-km downscaled	<u>0.526</u>	<u>0.059</u>	<u>0.018</u>	<u>0.021</u>	<u>0.719</u>	6
	AMSR-E	0.034	0.051	0.014	0.001	0.746	
	NLDAS	0.284	0.039	0.014	0.007	0.794	
	Micronet				0.021		

Table 5. Continued.

Day	Dataset	Slope	RMSE	Unbiased RMSE	Spatial SD	p value	Number of points	
			$\text{m}^3 \text{m}^{-3}$					
23 May 2004	1-km downscaled	<u>0.459</u>	<u>0.068</u>	<u>0.018</u>	<u>0.019</u>	<u>0.614</u>	8	
	AMSR-E	0.084	0.055	0.011	0.002	0.673		
	NLDAS	0.16	0.046	0.017	0.006	0.711		
	Micronet				0.02			
24 May 2004	1-km downscaled	<u>0.812</u>	<u>0.075</u>	<u>0.013</u>	<u>0.02</u>	<u>0.577</u>	9	
	AMSR-E	0.013	0.063	0.008	0.002	0.626		
	NLDAS	0.179	0.045	0.015	0.006	0.702		
	Micronet				0.017			
30 May 2004	1-km downscaled	<u>0.438</u>	<u>0.092</u>	–	0.009	<u>0.730</u>	5	
	AMSR-E	–	0.072	0.023	0.001	0.770		
	NLDAS	–0.002	0.043	–	–	0.842		
	Micronet				0.012			
3 July 2005	1-km downscaled	<u>0.237</u>	<u>0.066</u>	<u>0.064</u>	<u>0.028</u>	<u>0.747</u>	9	
	AMSR-E	0.039	0.049	0.058	0.005	0.775		
	NLDAS	0.095	0.061	0.05	0.004	0.832		
	Micronet				0.066			
8 July 2005	1-km downscaled	<u>0.224</u>	0.065	0.048	0.030	0.813	9	
	AMSR-E	0.08	0.039	0.039	0.004	0.669		
	NLDAS	0.168	0.021	0.044	0.010	0.810		
	Micronet				0.050			
12 July 2005	1-km downscaled	<u>0.032</u>	<u>0.049</u>	<u>0.029</u>	<u>0.025</u>	<u>0.864</u>	9	
	AMSR-E	–0.007	0.02	0.023	0.003	0.840		
	NLDAS	–0.013	0.033	0.03	0.005	0.785		
	Micronet				0.032			
17 July 2005	1-km downscaled	<u>0.176</u>	<u>0.05</u>	–	<u>0.026</u>	<u>0.825</u>	6	
	AMSR-E	0.228	0.033	–	0.002	0.871		
	NLDAS	0.16	0.057	–	0.002	0.806		
	Micronet				0.011			
22 July 2005	1-km downscaled	<u>–0.146</u>	<u>0.055</u>	<u>0.009</u>	<u>0.013</u>	<u>0.759</u>	9	
	AMSR-E	–0.027	0.029	0.015	0.005	0.813		
	NLDAS	–0.108	0.051	0.017	0.001	0.686		
	Micronet				0.009			
28 July 2005	1-km downscaled	<u>0.345</u>	<u>0.084</u>	–	<u>0.030</u>	<u>0.725</u>	5	
	AMSR-E	0.305	0.06	–	0.003	0.750		
	NLDAS	0.217	0.085	–	0.004	0.683		
	Micronet				0.020			
29 July 2005	1-km downscaled	<u>0.295</u>	<u>0.048</u>	0.012	<u>0.027</u>	<u>0.787</u>	9	
	AMSR-E	0.16	0.042	0.012	0.015	0.759		
	NLDAS	0.098	0.07	0.014	0.002	0.621		
	Micronet				0.005			
30 July 2005	1-km downscaled	<u>–0.204</u>	<u>0.08</u>	0.002	<u>0.034</u>	<u>0.036</u>	5	
	AMSR-E	–0.210	0.053	–	0.007	0.036		
	NLDAS	–0.238	0.056	–	0.002	0.036		
	Micronet				0.016			

Table 6. Monthly generalized comparison statistics between the 1-km downscaled, NLDAS and AMSR-E soil moisture compared to the Little Washita soil moisture observations for 3 mo. The 1-km downscaled values are underlined.

Day	Dataset	Slope	RMSE	Unbiased RMSE		Spatial SD	Number of points
				$\text{m}^3 \text{m}^{-3}$			
May 2004	1-km downscaled	<u>0.364</u>	<u>0.063</u>	<u>0.024</u>	<u>0.015</u>	64	
	AMSR-E	0.080	0.055	0.020	0.003		
	NLDAS	0.145	0.049	0.025	0.010		
	Micronet				0.027		
July 2005	1-km downscaled	<u>0.120</u>	<u>0.062</u>	<u>0.027</u>	<u>0.027</u>	61	
	AMSR-E	0.071	0.041	0.029	0.006		
	NLDAS	0.047	0.054	0.031	0.004		
	Micronet				0.028		
Total	1-km downscaled	<u>0.242</u>	<u>0.063</u>	<u>0.026</u>	<u>0.021</u>	125	
	AMSR-E	0.076	0.048	0.025	0.005		
	NLDAS	0.096	0.052	0.028	0.007		
	Micronet				0.028		

we show that the spatial standard variation of 1 km results is more systematically distributed than NLDAS and AMSR-E and also closer to the in situ soil moisture.

## Conclusions and Future Work

In this study, a soil moisture downscaling algorithm based on NLDAS derived regression relationship related daily surface temperature changes and average daily soil moisture was developed. This algorithm was applied using MODIS products of clear days during crop growing seasons (May, July, and August of 2004 and 2005) in Oklahoma. We used two sets of validation data, Oklahoma Mesonet and Little Washita Micronet soil moisture observations, to compare with the three estimates: 1-km downscaled soil moisture values, AMSR-E soil moisture values, and NLDAS soil moisture values. Statistical analysis was used to study the accuracy of the downscaling algorithm.

Several observations can be made using these results. First, the regression relationship supports our assumption that the surface temperature change depends on the wetness of the land surface and that the vegetation modulates this relationship. Second, the 1-km downscaled maps provide details on the soil moisture spatial distribution patterns in Oklahoma that are not available using AMSR-E product. The results also compare well with Oklahoma Mesonet soil moisture values. Third, considering Mesonet is biased wet (Illston et al., 2008), as is NLDAS (Mo et al., 2012), and that our system is based on NLDAS, we also have a slight bias. However, we are biased drier compared to Mesonet and NLDAS. This feature can be observed in Fig. 9a by comparing the distribution pattern among NLDAS, AMSR-E, and 1-km results, where more points of 1-km comparison plot are below the diagonal line than the other

two comparison plots. So the downscaled results are quite close to true values. Fourth, validation results of the three estimated soil moisture products against field observations from the Oklahoma Mesonet show that the slope for 1-km downscaled soil moisture are generally better and the spatial standard deviation is partially better than NLDAS and AMSR-E products. The overall spatial standard deviation of 1 km on August 2005 is closer to Mesonet, while on July 2005 and August 2005 is closer to either NLDAS or AMSR-E. Although the RMSE of 1-km downscaled soil moisture is poorer than the other soil moisture datasets, the unbiased RMSE of 1 km is better for some months. The *p* value of the Chi-squared goodness of fit test also shows that the comparison of field data with the 1-km downscaled map is statistically better than the NLDAS and AMSR-E products. Another advantage of the 1-km downscaled soil moisture result can be observed from comparisons with Little Washita Micronet data. The overall slope and spatial standard deviation using 1-km downscaled results in Table 6 are definitely better than the other two datasets, AMSR-E and NLDAS. In addition, the overall unbiased RMSE using 1-km downscaled is always better than NLDAS, while better than AMSR-E on July 2005. Although the results of Chi-squared test using data from the Micronet site and the three soil moisture datasets are poor, we did observe an improvement in the comparison of the results.

By comparing the scatter plots of spatial standard deviation, 1-km downscaled soil moisture demonstrates a better correlation with in situ soil moisture than NLDAS and AMSR-E soil moisture. Such trends are also noted when comparing with Micronet observations, where the NLDAS and AMSR-E comparisons are biased. Considering the slope and spatial standard deviation are two important variables that indicate similarity between observed and predicted measurements, this downscaling methodology not

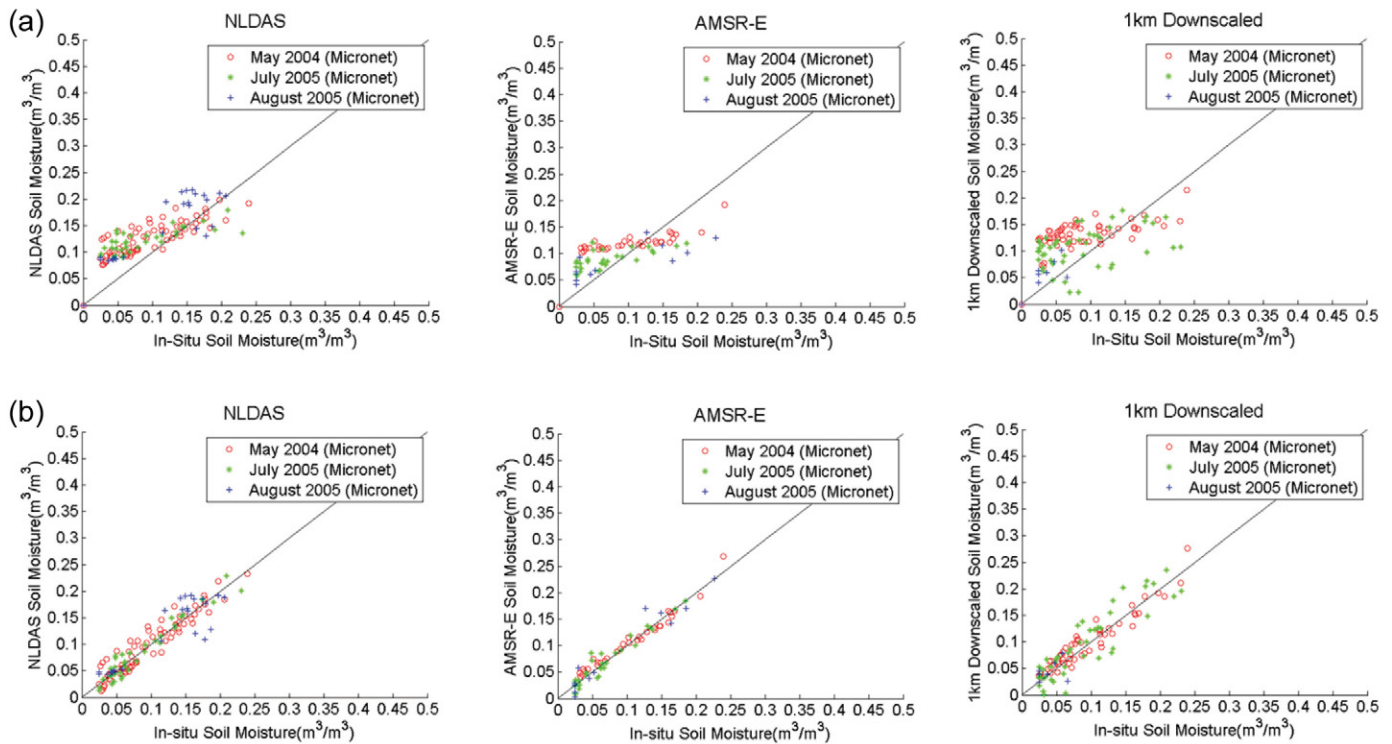


Fig. 9. (a) Overall scatter plots of NLDAS, AMSR-E, and 1-km soil moisture versus the Little Washita Micronet soil moisture observations for all the months. (b) Overall scatter plots of NLDAS, AMSR-E, and 1-km detrended soil moisture versus the Little Washita Micronet soil moisture observations for all the months.

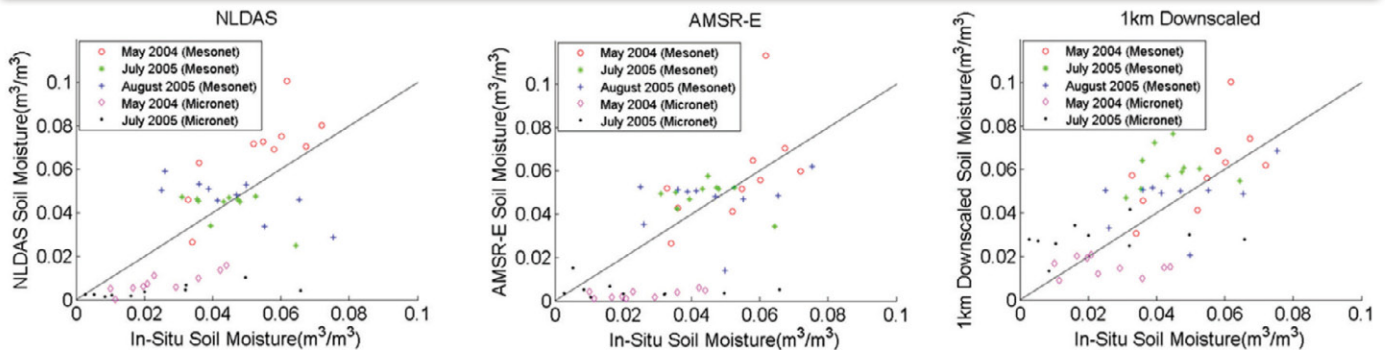


Fig. 10. Overall scatter plots of spatial standard deviation of NLDAS, AMSR-E, and 1-km soil moisture versus the Oklahoma Mesonet and Little Washita Micronet soil moisture observations for all the months.

only increases resolution and adds information about the spatial variability of the soil moisture within the AMSR-E estimates, but also preserves the average soil moisture. Any bias between the in situ observations and AMSR-E soil moisture will also be reflected in the disaggregated soil moisture estimates. We reported the unbiased RMSE estimates for different soil moisture products. However, the RMSE does not reflect the added value that the downscaled soil moisture provides about the spatial heterogeneity of soil moisture. The validation results proved that the soil moisture downscaling algorithm is applicable. In addition, if we compare our results with those reported in the literature and presented above (Table 1), we note that this analysis included a large area (the entire state of Oklahoma) and a longer period of time compared to some previous studies, which only

included shorter-term field experiments or smaller catchments, and our results show much lower RMSE. These include works by Rodríguez-Iturbe et al. (1995), Mohanty et al. (2000), Famiglietti et al. (2008), Heathman et al. (2012), and Minet et al. (2012) on spatial variability and uncertainty of soil moisture across scales as they relate to our research. In particular, studies reported by Mohanty et al. (2000) and Famiglietti et al. (2008) were based on observations made over the same study domain. These papers clearly demonstrated the scaling properties of soil moisture and the ability to observe soil moisture patterns across different scales. Remote sensing observations provide a spatially average estimate of soil moisture over the entire footprint.

Regarding these probable sources of uncertainty, several limitations still exist in this algorithm: (i) the MODIS temperature and NDVI products are often influenced by cloud coverage, so this method for downscaling is not appropriate for all weather conditions; (ii) the NDVI data comes from two sensors (AVHRR and MODIS) that were available for different time periods; (iii) the accuracy of NLDAS and AMSR-E soil moisture determines the accuracy of the 1-km downscaled soil moisture; (iv) only vegetation and temperature were used to develop this downscaling algorithm, and high spatial resolution data of these variables would be required for broader applications. This methodology is based on preserving the 25-km mean soil moisture, as is done for the AMSR-E soil moisture estimates. So, any overall day-to-day bias present in the AMSR-E soil moisture retrievals also will be present in the disaggregated 1-km estimates. Future work will combine this approach with our previous active-passive downscaling approach (Narayan et al., 2004), yielding an advantage that it can be applied in cloud-free as well as cloudy areas.

### Acknowledgments

We (Lakshmi and Fang) acknowledge the support of the NASA Terrestrial Hydrology Program (Manager Jared Entin) in carrying out this research.

### References

- Collatz, G., J.L. Botmouaz, D. Los, I.Y. Randall, and P.J. Sellers. 2000. A mechanism for the influence of vegetation on the response of the diurnal temperature range to changing climate. *Geophys. Res. Lett.* 27(20):3381–3384. doi:10.1029/1999GL010947
- Cosgrove, B.A., D. Lohmann, K.E. Mitchell, P.R. Houser, E.F. Wood, J.C. Schaake, A. Robock, C. Marshall, J. Sheffield, Q. Duan, L. Luo, R.W. Higgins, R.T. Pinker, J.D. Tarpley, and J. Meng. 2003. Real-time and retrospective forcing in the North American Land Data Assimilation System (NLDAS) project. *J. Geophys. Res.* 108(D22):8842. doi:10.1029/2002JD003118
- Cosh, M.H., T.J. Jackson, R. Bindlish, and J.H. Prueger. 2004. Watershed scale temporal and spatial stability of soil moisture and its role in validating satellite estimates. *Remote Sens. Environ.* 92(4):427–435. doi:10.1016/j.rse.2004.02.016
- Dai, A., and C. Deser. 1999. Diurnal and semidiurnal variations in global surface wind and divergence fields. *J. Geophys. Res.* 104(31):109–131.
- Das, N.N., D. Entekhabi, and E.G. Njoku. 2011. An algorithm for merging SMAP radiometer and radar data for high-resolution soil-moisture retrieval. *IEEE Trans. Geosci. Remote Sens.* 49(5):1504–1512. doi:10.1109/TGRS.2010.2089526
- De Fries, R.S., M. Hansen, J.R.G. Townshend, and R. Sohlberg. 1998. Global land cover classifications at 8 km spatial resolution: The use of training data derived from Landsat imagery in decision tree classifiers. *Int. J. Remote Sens.* 19(16):3141–3168. doi:10.1080/014311698214235
- Entekhabi, D., E. Njoku, P. O'Neill, M. Spencer, T. Jackson, J. Entin, E. Im, and K. Kellogg. 2008. The soil moisture active/passive mission (SMAP). In: *Geoscience and Remote Sensing Symposium, 2008. IGARSS 2008. IEEE International*, Vol. 3, p. III–1. doi:10.1109/IGARSS.2008.4779267
- Famiglietti, J.S., D. Ryu, A.A. Berg, M. Rodell, and T.J. Jackson. 2008. Field observations of soil moisture variability across scales. *Water Resour. Res.* 44:W01423. doi:10.1029/2006WR005804.
- Friedl, M.A., D.K. McIver, J.C.F. Hodges, X.Y. Zhang, D. Muchoney, A.H. Strahler, C.E. Woodcock, et al. 2002. Global land cover mapping from MODIS: Algorithms and early results. *Remote Sens. Environ.* 83(1–2):287–302. doi:10.1016/S0034-4257(02)00078-0
- Gillies, R.R., and T.N. Carlson. 1995. Thermal remote sensing of surface soil water content with partial vegetation cover for incorporation into climate models. *J. Appl. Meteorol.* 34(4):745–756. doi:10.1175/1520-0450(1995)034<0745:TRSOSS>2.0.CO;2
- Goetz, S.J. 1997. Multi-sensor analysis of NDVI, surface temperature and biophysical variables at a mixed grassland site. *Int. J. Remote Sens.* 18(1):71–94. doi:10.1080/014311697219286
- Heathman, G.C., M.H. Cosh, E. Han, T.J. Jackson, L. McKee, and S. McAfee. 2012. Field scale spatiotemporal analysis of surface soil moisture for evaluating point-scale in situ networks. *Geoderma* 170:195–205. doi:10.1016/j.geoderma.2011.11.004
- Heilman, J.L., and D.G. Moore. 1982. Evaluating near-surface soil moisture using Heat Capacity Mapping Mission data. *Remote Sens. Environ.* 12(2):117–121. doi:10.1016/0034-4257(82)90031-1
- Illston, B.G., J.B. Basara, C.A. Fiebrich, K.C. Crawford, E. Hunt, D.K. Fisher, R. Elliott, and K. Humes. 2008. Mesoscale monitoring of soil moisture across a statewide network. *J. Atmos. Ocean. Technol.* 25(2):167–182. doi:10.1175/2007JTECHA993.1
- Imaoka, K., M. Kachi, H. Fujii, H. Murakami, M. Hori, A. Ono, T. Igarashi, et al. 2010. Global Change Observation Mission (GCOM) for monitoring carbon, water cycles, and climate change. *Proc. IEEE* 98(5):717–734. doi:10.1109/JPROC.2009.2036869
- Jackson, T.J. 1993. III. Measuring surface soil moisture using passive microwave remote sensing. *Hydrol. Processes* 7(2):139–152. doi:10.1002/hyp.3360070205
- Jackson, T.J., D.M. Le Vine, A.Y. Hsu, A. Oldak, P.J. Starks, C.T. Swift, J.D. Isham, and M. Haken. 1999. Soil moisture mapping at regional scales using microwave radiometry: The Southern Great Plains Hydrology Experiment. *IEEE Trans. Geosci. Remote Sens.* 37:2136–2151.
- Jackson, T.J., A.J. Gasiewski, A. Oldak, M. Klein, E.G. Njoku, A. Yevgrafov, S. Christiani, and R. Bindlish. 2002. Soil moisture retrieval using the C-band polarimetric scanning radiometer during the Southern Great Plains 1999 Experiment. *IEEE Trans. Geosci. Remote Sens.* 40:2151–2161. doi:10.1109/TGRS.2002.802480
- Jackson, T.J., M.H. Cosh, R. Bindlish, P.J. Starks, D.D. Bosch, M. Seyfried, D.C. Goodrich, M.S. Moran, and J. Du. 2010. Validation of advanced microwave scanning radiometer soil moisture products. *IEEE Trans. Geosci. Remote Sens.* 48:4256–4272. doi:10.1109/TGRS.2010.2051035
- Justice, C.O., J.R.G. Townshend, E.F. Vermote, E. Masuoka, R.E. Wolfe, N. Saleous, D.P. Roy, and J.T. Morisette. 2002. An overview of MODIS Land data processing and product status. *Remote Sens. Environ.* 83(1–2):3–15. doi:10.1016/S0034-4257(02)00084-6
- Karl, T.R., G. Kukla, and J. Gavin. 1984. Decreasing diurnal temperature range in the United States and Canada from 1941 through 1980. *J. Clim. Appl. Meteorol.* 23(11):1489–1504. doi:10.1175/1520-0450(1984)023<1489:DD TRIT>2.0.CO;2
- Kim, J., and T.S. Hogue. 2012. Improving spatial soil moisture representation through integration of AMSR-E and MODIS products. *IEEE Trans. Geosci. Remote Sens.* 50(2):446–460. doi:10.1109/TGRS.2011.2161318
- Knight, J.F., et al. 2006. Regional scale land cover characterization using MODIS-NDVI 250 m multi-temporal imagery: A phenology-based approach. *GISci. Remote Sens.* 43(1):1–23. doi:10.2747/1548-1603.43.1.1
- Kurc, S.A., and E.E. Small. 2004. Dynamics of evapotranspiration in semiarid grassland and shrubland ecosystems during the summer monsoon season, central New Mexico. *Water Resour. Res.* 40:W09305. doi:10.1029/2004WR003068
- Lakshmi, V., S. Hong, E.E. Small, and F. Chen. 2011. The influence of the land surface on hydrometeorology and ecology: New advances from modeling and satellite remote sensing. *Hydrol. Res.* 42(2–3):95–112. doi:10.2166/nh.2011.071
- Lakshmi, V., E.F. Wood, and B.J. Choudhury. 1997. Evaluation of Special Sensor Microwave/Imager satellite data for regional soil moisture estimation over the Red River Basin. *J. Appl. Meteorol.* 36(10):1309–1328. doi:10.1175/1520-0450(1997)036<1309:EOSSMI>2.0.CO;2
- Land Long Term Data Record (LTDR). 2011. AVHRR data. <http://ltdr.nascom.nasa.gov/> (accessed 2011). NASA, Goddard Space Center.
- Lohmann, D., K.E. Mitchell, P.R. Houser, E.F. Wood, J.C. Schaake, A. Robock, B.A. Cosgrove, et al. 2004. Streamflow and water balance intercomparisons of four land surface models in the North American Land Data Assimilation System project. *J. Geophys. Res.* 109(D7):D07591. doi:10.1029/2003JD003517
- Luo, L., A. Robock, K.E. Mitchell, P.R. Houser, E.F. Wood, J.C. Schaake, D. Lohmann, et al. 2003. Validation of the North American Land Data Assimilation System (NLDAS) retrospective forcing over the southern Great Plains. *J. Geophys. Res.* 108(D22):8843. doi:10.1029/2002JD003246
- Mallick, K., B.K. Bhattacharya, and N.K. Patel. 2009. Estimating volumetric surface moisture content for cropped soils using a soil wetness index based on surface temperature and NDVI. *Agric. For. Meteorol.* 149(8):1327–1342. doi:10.1016/j.agrformet.2009.03.004
- McPherson, R.A., C.A. Fiebrich, K.C. Crawford, J.R. Kilby, D.L. Grimsley, J.E. Martinez, J.B. Basara, et al. 2007. Statewide monitoring of the mesoscale environment: A technical update on the Oklahoma Mesonet. *J. Atmos. Ocean. Technol.* 24(3):301–321. doi:10.1175/JTECH1976.1
- Merlin, O., A. Al Bitar, J.P. Walker, and Y. Kerr. 2009. A sequential model for disaggregating near-surface soil moisture observations using multi-resolution thermal sensors. *Remote Sens. Environ.* 113(10):2275–2284. doi:10.1016/j.rse.2009.06.012
- Merlin, O., A. Al Bitar, J.P. Walker, and Y. Kerr. 2010. An improved algorithm for disaggregating microwave-derived soil moisture based on red, near-infrared and thermal-infrared data. *Remote Sens. Environ.* 114(10):2305–2316. doi:10.1016/j.rse.2010.05.007

- Merlin, O., J.P. Walker, A. Chehbouni, and Y. Kerr. 2008a. Towards deterministic downscaling of SMOS soil moisture using MODIS derived soil evaporative efficiency. *Remote Sens. Environ.* 112(10):3935–3946. doi:10.1016/j.rse.2008.06.012
- Merlin, O., A. Chehbouni, J.P. Walker, R. Panciera, and Y.H. Kerr. 2008b. A simple method to disaggregate passive microwave-based soil moisture. *IEEE Trans. Geosci. Remote Sens.* 46(3):786–796. doi:10.1109/TGRS.2007.914807
- Merlin, O., C. Rudiger, A. Al Bitar, P. Richaume, J.P. Walker, and Y.H. Kerr. 2012. Disaggregation of SMOS soil moisture in Southeastern Australia. *IEEE Trans. Geosci. Remote Sens.* 50(5):1556–1571. doi:10.1109/TGRS.2011.2175000
- Minacapilli, M., M. Iovino, and F. Blanda. 2009. High resolution remote estimation of soil surface water content by a thermal inertia approach. *J. Hydrol.* 379(3–4):229–238. doi:10.1016/j.jhydrol.2009.09.055
- Minet, J., P. Bogaert, M. Vanclooster, and S. Lambot. 2012. Validation of ground penetrating radar full waveform inversion for field scale soil moisture mapping. *J. Hydrol.* 424–425:112–123. doi:10.1016/j.jhydrol.2011.12.034
- Mitchell, K.E., D. Lohmann, P.R. Houser, E.F. Wood, J.C. Schaake, A. Robock, B.A. Cosgrove, et al. 2004. The multi-institution North American Land Data Assimilation System (NLDAS): Utilizing multiple GCIIP products and partners in a continental distributed hydrological modeling system. *J. Geophys. Res.* 109(D7). doi:10.1029/2003JD003823.
- Mladenova, Iliana, Venkat Lakshmi, Thomas J. Jackson, Jeffrey P. Walker, Olivier Merlin, and Richard AM de Jeu. 2011. Validation of AMSR-E soil moisture using L-band airborne radiometer data from National Airborne Field Experiment 2006. *Remote Sens. Environ.* 115:2096–2103. doi:10.1016/j.rse.2011.04.011
- Mo, K.C., L.-C. Chen, S. Shukla, T.J. Bohn, and D.P. Lettenmaier. 2012. Uncertainties in North American land data assimilation systems over the contiguous United States. *J. Hydrometeorol.* 13:996–1009. doi:10.1175/JHM-D-11-0132.1
- Mohanty, B.P., J.S. Famiglietti, and T.H. Skaggs. 2000. Evolution of soil moisture spatial structure in a mixed vegetation pixel during the Southern Great Plains 1997 (SGP97) hydrology experiment. *Water Resour. Res.* 36:3675–3686. doi:10.1029/2000WR900258
- Myneni, R.B., F.G. Hall, P.J. Sellers, and A.L. Marshak. 1995. The interpretation of spectral vegetation indexes. *IEEE Trans. Geosci. Remote Sens.* 33(2):481–486. doi:10.1109/36.377948
- Myneni, R.B., S. Hoffman, Y. Knyazikhin, J.L. Privette, J. Glassy, Y. Tian, Y. Wang, et al. 2002. Global products of vegetation leaf area and fraction absorbed PAR from year one of MODIS data. *Remote Sens. Environ.* 83(1–2):214–231. doi:10.1016/S0034-4257(02)00074-3
- Narayan, U., V. Lakshmi, and E.G. Njoku. 2004. A simple algorithm for spatial disaggregation of radiometer derived soil moisture using higher resolution radar observations. In: *Geoscience and Remote Sensing Symposium, 2004. IGARSS'04. Proceedings. 2004 IEEE International*, Vol. 3, p. 1877–1879. doi:10.1109/IGARSS.2004.1370706
- Narayan, U., and V. Lakshmi. 2008. Characterizing subpixel variability of low resolution radiometer derived soil moisture using high resolution radar data. *Water Resour. Res.* 44(6). doi:10.1029/2006WR005817
- National Aeronautics and Space Administration (NASA). 2011. National Space Science Data Center. NSSIDC ID: 1978–041A. <http://nssdc.gsfc.nasa.gov/nmc/spaccraftDisplay.do?id=1978-041A> (accessed 2011).
- Njoku, E.G., and D. Entekhabi. 1996. Passive microwave remote sensing of soil moisture. *J. Hydrol.* 184(1–2):101–129. doi:10.1016/0022-1694(95)02970-2
- Njoku, E.G., T.J. Jackson, V. Lakshmi, T.K. Chan, and S.V. Nghiem. 2003. Soil moisture retrieval from AMSR-E. *IEEE Trans. Geosci. Remote Sens.* 41(2):215–229. doi:10.1109/TGRS.2002.808243
- Njoku, E.G., and L. Li. 1999. Retrieval of land surface parameters using passive microwave measurements at 6–18 GHz. *IEEE Trans. Geosci. Remote Sens.* 37(1):79–93. doi:10.1109/36.739125
- Njoku, E.G., and S.K. Chan. 2006. Vegetation and surface roughness effects on AMSR-E land observations. *Remote Sens. Environ.* 100(2):190–199. doi:10.1016/j.rse.2005.10.017
- North American Land Data Assimilation Systems (NLDAS). 2011. NLDAS data. <http://ldas.gsfc.nasa.gov/> (accessed 2011).
- Pan, M., E.F. Wood, D.B. McLaughlin, D. Entekhabi, and L. Luo. 2009. A multiscale ensemble filtering system for hydrologic data assimilation. Part I: Implementation and synthetic experiment. *J. Hydrometeorol.* 10(3):794–806. doi:10.1175/2009JHM1088.1
- Parada, L.M., and X. Liang. 2004. Optimal multiscale Kalman filter for assimilation of near-surface soil moisture into land surface models. *J. Geophys. Res.* 109(D24):D24109. doi:10.1029/2004JD004745
- Piles, M., A. Camps, M. Vall-Llossera, I. Corbella, R. Panciera, C. Rudiger, Y.H. Kerr, and J. Walker. 2011. Downscaling SMOS-derived soil moisture using MODIS visible/infrared data. *IEEE Trans. Geosci. Remote Sens.* 49(9):3156–3166. doi:10.1109/TGRS.2011.2120615
- Rodríguez-Iturbe, I., G.K. Vogel, R. Rigon, D. Entekhabi, F. Castelli, and A. Rinaldo. 1995. On the spatial organization of soil moisture fields. *Geophys. Res. Lett.* 22(20):2757–2760. doi:10.1029/95GL02779
- Robock, A., L. Luo, E.F. Wood, F. Wen, K.E. Mitchell, P.R. Houser, J.C. Schaake, et al. 2003. Evaluation of the North American Land Data Assimilation System over the southern Great Plains during the warm season. *J. Geophys. Res.* 108(no. D22):8846. doi:10.1029/2002JD003245
- Sahoo, A.K., G.J.M. De Lannoy, R.H. Reichle, and P.R. Houser. 2012. Assimilation and downscaling of satellite observed soil moisture over the Little River Experimental Watershed in Georgia, USA. *Adv. Water Resour.* 52:19–33. doi:10.1016/j.advwatres.2012.08.007
- Sandholt, I., K. Rasmussen, and J. Andersen. 2002. A simple interpretation of the surface temperature/vegetation index space for assessment of surface moisture status. *Remote Sens. Environ.* 79(2–3):213–224. doi:10.1016/S0034-4257(01)00274-7
- Schaake, J.C., Q. Duan, V. Koren, K.E. Mitchell, P.R. Houser, E.F. Wood, A. Robock, et al. 2004. An intercomparison of soil moisture fields in the North American Land Data Assimilation System (NLDAS). *J. Geophys. Res.* 109(D1):D01S90. doi:10.1029/2002JD003309
- Schmugge, T., P. Gloersen, T. Wilheit, and F. Geiger. 1974. Remote sensing of soil moisture with microwave radiometers. *J. Geophys. Res.* 79(2):317–323. doi:10.1029/JB079i002p00317
- Tucker, C.J. 1979. Red and photographic infrared linear combinations for monitoring vegetation. *Remote Sens. Environ.* 8(2):127–150. doi:10.1016/0034-4257(79)90013-0
- van Genuchten, M.Th. 1980. A closed-form equation for predicting the hydraulic conductivity of unsaturated soils. *Soil. Sci. Soc. Am. J.* 44:892–898.
- Wan, Z., and Z.-L. Li. 1997. A physics-based algorithm for retrieving land-surface emissivity and temperature from EOS/MODIS data. *IEEE Trans. Geosci. Remote Sens.* 35(4):980–996. doi:10.1109/36.602541
- Zhang, X., et al. 2003. Monitoring vegetation phenology using MODIS. *Remote Sens. Environ.* 84(3):471–475. doi:10.1016/S0034-4257(02)00135-9
- Zhou, Y., D. McLaughlin, D. Entekhabi, and G.-H.C. Ng. 2008. An ensemble multiscale filter for large nonlinear data assimilation problems. *Mon. Weather Rev.* 136(2):678–698. doi:10.1175/2007MWR2064.1